

PERFORMANCE ANALYSIS OF PRINTED ARRAY ANTENNAS
FOR 5G MOBILE COMMUNICATIONS

Thesis Submitted to
School of Electrical and Computer Engineering
ADDIS ABABA UNIVERSITY

In Partial Fulfillment of the Requirements for the Degree of Master of Science in
Communication Engineering

By
Muzev Tsigab
Advisor
Dr. Murad Ridwan



Addis Ababa, Ethiopia

October, 2021

DECLARATION

I, the undersigned, declare that the thesis comprises my own work in compliance with internationally accepted practices; I have fully acknowledged and referred all materials used in this thesis work.

Muzey Tsigab _____

Name

Signature

Addis Ababa _____

Place

Date of Submission

This thesis has been submitted for examination with my approval as a university advisor.

Dr. Murad Ridwan _____

Advisor

Signature



Addis Ababa University

Addis Ababa Institute of Technology

School of Electrical and Computer Engineering

Performance Analysis of Printed Array Antennas for 5G Mobile Communications

By: Muzey Tsigab

APPROVED BY BOARD OF EXAMINERS

_____	_____
Chairman Dept. of Graduate Committee	Signature
Dr. Murad Ridwan _____	_____
Advisor	Signature
_____	_____
Internal Examiner	Signature
_____	_____
External Examiner	Signature

ABSTRACT

Nowadays with the limited spectrum bands the mobile operators have been challenged to deliver multimedia applications with higher data rates, low latency and better quality of service of mobile communications to a growing number of users. This has led to a big number of inventions and technology advancement in past decades which is the prime goals of the upcoming 5th generation (5G) mobile networks. The millimeter wave (mmWave) is a suitable candidate for 5G with its high frequency range from 30 GHz up to 300 GHz. This thesis aims to design, analyze, simulate and compare the single and array elements of printed dipole, microstrip patch and planar inverted-F (PIFA) antennas regarding to their performances at the same operating frequency of 28 GHz using computer simulated technology (CST) microwave studio electromagnetic simulator. The comparison is based on simulated results of radiation pattern, gain, directivity, VSWR, return loss and efficiency.

Based on the results obtained 4×1 array antennas have maximum gain and directivity of 9.87 dBi and 10.12 dBi for printed dipole antenna, 12.09 dBi and 12.37 dBi for microstrip patch antenna, and 9.79 dBi and 9.812 dBi for PIFA, respectively. The VSWR and return loss value, respectively, is found to be 2.4 and -7.57 dB for printed dipole array antenna, 1.09 and -27.37 dB for microstrip patch array antenna, and 2.6 and -6.5 dB for array of PIFA. The radiation efficiency for printed dipole array antenna is -0.248, for microstrip patch array antenna is -0.275, and for array of PIFA is -0.18. In this regard, the analysis shows that the microstrip patch antenna is quite capable of achieving the highest performances and represent an obvious choice for mobile applications. Moreover, to achieve an optimum design parameter the microstrip patch array antenna is also simulated with varying values of the substrate height, substrate thickness, patch length and patch width. The effect of these parameters on antenna performance is analyzed.

Keywords: Millimeter Wave, PIFA, Printed Dipole, Patch, CST, 28 GHz, Array Antenna

ACKNOWLEDGMENTS

First and foremost, I would like to thank the almighty God for giving me the strength and patience to undertake this thesis.

I would like to express my heartfelt and sincere gratitude to my supervisor, Dr. Murad Ridwan for the unstinting guidance, motivation, consistent support, and valuable time given throughout this thesis.

Finally, I would like to give special thanks to my family for their unconditional support and encouragement throughout my study and to my friends who have been a pillar of support in all terms to bring out this work.

TABLE OF CONTENTS

DECLARATION	i
ABSTRACT	iii
ACKNOWLEDGMENTS	v
LIST OF FIGURES	viii
LIST OF TABLES	x
LIST OF ABBREVIATIONS	xi
LIST OF SYMBOLS	xiii
CHAPTER I. INTRODUCTION	1
1.1 Problem Statement	1
1.2 Objectives	3
1.2.1 General Objective	3
1.2.2 Specific Objectives	3
1.3 Methodology	3
1.4 Literature Review	4
1.5 Outline of the Thesis	6
CHAPTER II. ANTENNA PARAMETERS AND ANTENNA THEORY	7
2.1 Overview of Antenna Parameters	7
2.1.1 Radiation Pattern	7
2.1.2 Directivity	8
2.1.3 Gain	9
2.1.4 Antenna Efficiency	10
2.1.5 Input Impedance	10
2.1.6 Return Loss	13
2.1.7 S-parameters	14
2.1.8 Bandwidth	14
2.2 Types of Antennas	16
2.2.1 Printed Dipole Antenna	16
2.2.2 Microstrip Patch Antenna	17
2.2.3 Planar Inverted-F Antenna (PIFA)	23
CHAPTER III. DESIGN AND ANALYSIS	26
3.1 Designing of Printed Dipole Antenna	26
3.2 Designing of Microstrip Patch Antenna	29
3.3 Designing of Planar Inverted-F Antenna (PIFA)	35
CHAPTER IV. SIMULATION RESULTS	38
4.1 Simulation Result for Printed Dipole Antenna	38

4.2	Simulation Result for Microstrip Patch Antenna	41
4.3	Simulation Result for Planar Inverted-F Antenna	44
CHAPTER V. CONCLUSION AND RECOMMENDATION FOR FUTURE WORK		56
5.1	Conclusion	56
5.2	Recommendation for Future Work	57
BIBLIOGRAPHY		58
APPENDIX		61

LIST OF FIGURES

1.1	Left: The total scan pattern of the DRA array. Right: The total scan pattern of the SIW array [1]	4
2.1	Spherical Coordinate Systems for Antenna Analysis [2]	8
2.2	Structure of Printed Dipole Antenna	17
2.3	Structure of Microstrip Patch Antenna [3]	18
2.4	Microstrip Line Feed [3]	21
2.5	Coaxial Feed [3]	22
2.6	Aperture Coupled Feed [3]	23
2.7	Proximity Coupling Feed [3]	24
2.8	Structure of PIFA [4]	24
3.1	Designed single printed dipole antenna on CST MWS	26
3.2	Designed printed dipole array antenna on CST MWS	28
3.3	Designed single element microstrip Antenna	30
3.4	Microstrip series feed network [5]	34
3.5	4×1 corporate feed microstrip array antenna using CST model	35
3.6	Designed single PIFA on CST MWS	35
3.7	Geometrical configuration of four-element PIFA array antenna	37
4.1	S-parameter for single printed dipole antenna	39
4.2	S-parameter for 4×1 printed dipole array antenna	39
4.3	VSWR plot of single printed dipole antenna	40
4.4	VSWR plot of 4×1 printed dipole array antenna	40
4.5	3-D far-field radiation pattern of single printed dipole antenna	41
4.6	3-D far-field gain of single printed dipole antenna	41

4.7	3-D far-field radiation pattern of 4×1 printed dipole array antenna	42
4.8	3-D far-field gain of 4×1 printed dipole array antenna	42
4.9	3-D polar plot of 4×1 printed dipole array antenna	43
4.10	S-parameter for single microstrip patch antenna	43
4.11	S-parameter for 4×1 microstrip patch array antenna	44
4.12	VSWR plot of single microstrip patch antenna	44
4.13	VSWR plot of 4×1 microstrip patch array antenna	45
4.14	3-D far-field radiation pattern of single microstrip patch antenna	45
4.15	3-D far-field gain of single microstrip patch antenna	46
4.16	3-D far-field radiation pattern of 4×1 microstrip patch array antenna	46
4.17	3-D far-field gain of 4×1 microstrip patch array antenna	47
4.18	3-D polar plot of 4×1 microstrip patch array antenna	47
4.19	S-parameter for single PIFA antenna	48
4.20	S-parameter for 4×1 PIFA array antenna	48
4.21	VSWR plot of single PIFA antenna	49
4.22	VSWR plot of 4×1 PIFA array antenna	49
4.23	3-D far-field radiation pattern of single PIFA	50
4.24	3-D far-field gain of single PIFA	50
4.25	3-D far-field radiation pattern of 4×1 PIFA array antenna	52
4.26	3-D far-field gain of 4×1 PIFA array antenna	52
4.27	3-D polar plot of 4×1 PIFA array antenna	53

LIST OF TABLES

4.1	Comparison of antennas performance	51
4.2	Effect of substrate material	51
4.3	Effect of the patch width	53
4.4	Effect of the patch length	54
4.5	Effect of the substrate thickness	55

LIST OF ABBREVIATIONS

3D	Three-dimensional
5G	5th generation
AAIT	Addis Ababa Institute of Technology
Approx.	Approximately
BW	Band width
CAD	Computer aided design
CST	Computer simulation technology
dB	Decibel
DBS	Direct broadcasting satellite
Dir.	Directivity
DRA	Dielectric resonator antenna
ECE	Electrical and computer engineering
EDA	Electronic design automation
EM	Electromagnetic
EMC	Electromagnetic compatibility
EMI	Electromagnetic interference
GHz	Gigahertz
GPS	Global positioning systems
GSM	Global system for mobile communications
HF	Higher frequency
HFSS	High-frequency structure simulator
HPBW	Half power beam width
IEEE	Institute of electrical and electronics engineers

LTE	Long term evolution
LOS	Line of sight
MHz	Megahertz
MIMO	Multiple input multiple output
Mm	Millimeters
mm-Wave	Millimeter-wave
MWS	Microwave studio
PCB	Printed circuit board
PIFA	Planar inverted F antenna
Rad. effic.	Radiation efficiency
RF	Radio frequency
RFID	Radio frequency identification
SDR	Satellite digital radio
SIW	Substrate integrated waveguide
SNR	Signal to noise ratio
SPICE	Simulation program with integrated circuit emphasis
Tot. effic.	Total Efficiency
VSWR	Voltage standing wave ratio
WCS	Wireless communications service
WiMAX	Worldwide interoperability for microwave access
WLAN	Wireless local area networks

LIST OF SYMBOLS

η	Antenna efficiency
c	Velocity of light in free space
d	Distance between the antennas
ϵ_r	Relative dielectric constant of substrate
ϵ_{reff}	Effective dielectric constant
e_0	Total efficiency
e_r	Reflection efficiency
e_c	Conduction efficiency
e_d	Dielectric efficiency
f_0	Operating frequency
g	Feeding gap
G	Gain of the antenna
G_R	Gain for receiving antenna
G_T	Gain for transmitting antenna
h	Height of the dielectric substrate
h_s	Height of shortening plate
λ	Operating wavelength/Lambda
L	Length of the patch antenna
L_g	Length of ground plane
L_{eff}	Effective length of patch
L_p	Path loss
P_{in}	Total input power
P_R	Power for receiving antenna

P_{rad}	Total power radiated
P_T	Power for transmitting antenna
R_{in}	Antenna resistance at the terminals
R_s	Source resistance
t	Patch thickness
U	Radiation intensity of the antenna
U_0	Radiation intensity of an isotropic source
V_r	Amplitude of the reflected wave
V_i	Amplitude of the incident wave
W	Width of patch antenna
W_g	Width of ground plane
W_s	Width of the shortening plate
X_{in}	Antenna reactance at the terminals
X_s	Source reactance
Z_{in}	Antenna impedance at the terminals
Z_s	Source impedance
$\ \Gamma\ $	Reflection coefficient

CHAPTER I

INTRODUCTION

An antenna is a device that is designed for radiating or/and receiving electromagnetic energy. Basically, everything emanates electromagnetic waves however antennas are designed to have a good performance at specific frequencies and bandwidths [2, 6]. Antennas are very significant elements of communication systems since they are utilized in transmitting and receiving signals. At the time when an antenna is fed by a specific signal, the emitted radiation is distributed in the space in a particular way. It can be said that antennas are the backbone and nearly everything in the wireless communication without which the world could have not reached at this time of innovation [7]. The growing demand for higher data rates, low latency, and better quality of service of mobile communications have led to a big number of inventions and technology advancement in past decades which is the prime goals of the upcoming 5th generation (5G) mobile networks [8]. The everlasting antenna theory is not going to be changed but the upcoming 5G will reform old standards and unforeseen antenna inventions will see the daylight. The underlying exploration on the empowering innovations for the upcoming 5th generation network (5G) is progressively proposing the utilization of the millimeter-wave (mm-Wave) spectrum. The mmWave is a suitable candidate for 5G with its high frequency range from 30 up to 300 GHz. Accordingly, the use of mm-Wave spectrum will require various design of antennas in 5G communication systems. 5G will achieve improvements in wanted characteristics like throughput, coverage, capacity and reliability [8, 9]. Reaching the 5G performance requires tight antenna arrays where separations between antenna elements are short.

1.1 Problem Statement

For supporting high quality multimedia applications in future smart-phones, the massive increment in mobile data rates creates new challenges in regards to the development of the 5th generation mobile system. Due to shortage of frequency spectrum below 6 GHz, bands at the mmWave frequencies have been widely suggested as candidates, as the considerably larger bandwidths could be exploited to increase the capacity and enable the user to experience several gigabits per second data rates [1].

However, moving from the much lower cellular carrier frequencies used today (700 MHz - 2.6 GHz) up towards the mmWave bands results in a much higher free space path loss, as can be seen from equation 1.1 below.

In free space, the wave is not reflected or absorbed [10]. The free space path loss model is used to predict received signal strength when the transmitter and receiver have a clear, unobstructed line of sight path between them. The free space power received by a receiver antenna from a radiating transmitter antenna at a path length d is given by the "Friis Equation" as written in equation 1.1.

$$P_r = P_t G_t G_r (\lambda / 4\pi d)^2 \quad (1.1)$$

Where, P_r is the received power, P_t is the transmitted power, d is the distance between the antennas, G_t is the transmitter antenna gain, G_r is the receiver antenna gain, λ is the wavelength of the antenna and d is the distance between transmitting and receiving antennas. All terms are in linear units, not dB.

Expressing in decibel (dB) we get,

$$P_r(dBm) = P_t(dBm) + G_t(dB) + G_r(dB) - L_p(dB) \quad (1.2)$$

Where

$$L_p(dB) = 20 \log(4\pi d / \lambda)$$

This term is called the "free space path loss".

The free space path loss will be much higher for the higher frequency band than current mobile networks due to the shorter wavelength. Subsequently, antenna gains of both in base stations and portable terminals should be expanded to compensate the higher path loss without expending any more power [11].

1.2 Objectives

1.2.1 General Objective

The general objective of this thesis is to design, demonstrate and analyze the performance of single element and arrays of printed antenna at 28 GHz.

1.2.2 Specific Objectives

The specific objectives of this thesis are stated as follows:

To design, analyze and simulate the single printed dipole, PIFA, and the patch antennas operating at 28 GHz.

To design, analyze and simulate the 4×1 printed dipole, PIFA, and the patch array antennas operating at 28 GHz.

To compare and contrast the performance of the three printed array antennas.

To select an antenna, involving the standard antenna parameters, which has better radiation pattern, gain, directivity and efficiency, thus, best suited for the fifth generation of mobile communications.

1.3 Methodology

The study of this thesis involves the following steps to achieve its objectives.

Literature Review and Data collection: Related articles, research papers, and software's are reviewed to strengthen the study.

System Modeling and Implementation: Determine antenna parameters, analyze and simulate the different types of antennas to find the different parameters like gain, directivity, VSWR, return loss and efficiency using CST Microwave Studio (MWS) software at 28 GHz frequency, which is one of the expected frequencies to be used in 5G.

Interpretation and Discussion: From the simulated results compare the approximated values of gain, directivity and efficiency provided by the different types of printed antenna arrays. Based on the comparison and evaluation of the different radiation characteristics, conclude which types of antennas are best suited to the fifth generation of mobile communications.

1.4 Literature Review

Many research papers and articles have been published on performance analysis of different antennas regarding their characteristics of total scan pattern, gain, directivity, coverage efficiency, return loss or VSWR separately but not comprehensively all at once. For example, in [1] the objective was to analyze the performance of the total scan pattern and coverage efficiency as parameters of evaluation for an open-ended substrate integrated waveguide (SIW), a rectangular patch and a dielectric resonator antenna (DRA) operating at 28 GHz, regardless of the other parameters. Different sub-array schemes were introduced to illustrate the advantages of a pattern diversity and the coverage efficiency can be enhanced. The arrays considered were 8×1 configurations with element spacing slightly less than half a free space wavelength. The maximum gain for the 8×1 array was 14.5, 14.9 and 12.5 dBi for the patch, DRA and SIW configuration, respectively. The total scan pattern of the DRA and SIW array respectively were depicted in Figure 1.1.

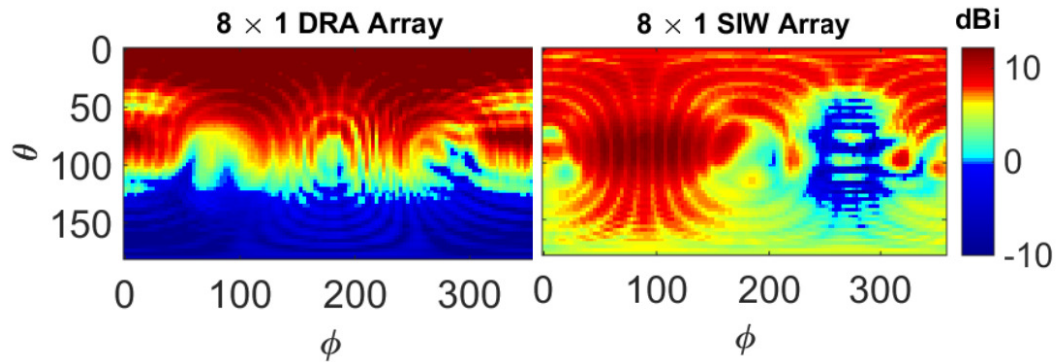


Figure 1.1: Left: The total scan pattern of the DRA array. Right: The total scan pattern of the SIW array [1]

In [12] for investigating the performance, the total scan pattern of the array configuration along with its particular coverage efficiency were basic to consider so as to compare different antenna designs and topology approaches with each other. This paper proposed an approach of analyzing performance of utilized phased array antennas operating at millimeter wave (mmWave) frequencies for future cellular networks. Two different antenna designs were considered; an aperture-coupled rectangular patch and a quarter-wavelength notch. Potential designs need to be cheap to manufacture and integrated on a very limited space in the smart-phone. Along these lines, the antenna types are chosen because of their small size; in terms of half a wavelength in the substrate, which enables array implementation at the desired operating frequency, 15 GHz. The arrays are 4×1 configurations with element spacing slightly less than half a free space wavelength. All simulations were performed in CST Microwave Studio (MWS). From the simulated results the maximum absolute gain achieved was 9.9 dBi and 10.4 dBi for the notch array and the patch array, respectively. The radiation efficiency was 85% for the patch and 87% for the notch arrays. The patch array has higher directional element radiation pattern, but less radiation efficiency than that of the notch array.

On the other hand, in [13] the parameters of evaluation for comparison the simulated results of rectangular patch and PIFA antennas were return loss and VSWR using Ansoft HFSS with an operating frequency 2.4 GHz. The return loss values for patch and PIFA antenna, respectively, were obtained as -30.65 dB and -41.04 dB. The values for VSWR for patch and PIFA antenna were obtained as 0.51 and 0.15, respectively. The resulting impedance bandwidth of these antennas can support WCS and SDR bands. From the results, it was revealed that PIFA antenna shows better results for return loss values than patch antenna. This thesis aims to design, analyze and compare the performance of printed

dipole antenna, microstrip patch antenna and planar inverted-f antenna at an operating frequency of 28 GHz. The parameters of evaluation for comparison the simulated results of these antennas are gain, directivity, efficiency, return loss and VSWR comprehensively all at the same time using CST microwave studio electromagnetic simulator.

1.5 Outline of the Thesis

This thesis is composed of five chapters and the overview of each chapter is as follows:

Chapter 1: The introduction, problem statement, objective, methodology and literature reviews on the printed array antennas are discussed on this chapter.

Chapter 2: This chapter presents the fundamental antenna parameters, review on the theory of printed dipole antenna, microstrip patch antenna and planar inverted-F antenna.

Chapter 3: This chapter discusses the analysis and design of the printed array antennas which operates at mm-wave frequency specifically at 28 GHz.

Chapter 4: The simulation results obtained on both single element and four by one elements of the printed array antennas are discussed and compared in this chapter.

Chapter 5: Conclusion of the thesis and suggestions for future work are presented in this final chapter.

CHAPTER II

ANTENNA PARAMETERS AND ANTENNA THEORY

2.1 Overview of Antenna Parameters

Antenna parameters are used to describe the performance of an antenna when designing and measuring antennas. In this section, characteristics such as the directivity, bandwidth, radiation pattern, gain, efficiency, input impedance, return loss and s-parameters are explained.

2.1.1 Radiation Pattern

The radiation pattern is expressed as the relative power of a radiated field in different directions of an antenna. It is characterized as "the spatial distribution of a quantity that characterizes the electromagnetic field generated by antenna". Radiation pattern can be a two or three dimensional spatial distribution of power flux density, radiation intensity, field strength, directivity, phase or polarization. Radiation pattern is a function of the observer's position along a path or surface of constant radius and goes through a direction at which maximum radiation occurs. For the most part, the spherical coordinate system is utilized to picture the radiation pattern. A two dimensional pattern can be a function of the elevation angle, θ , at constant azimuth angle, ϕ , or a function of ϕ at constant θ value [14]. The spherical coordinate system is shown in Figure 2.1.

Antenna's radiation fields can be divided into three regions, a reactive near-field, radiating near-field and far-field. The radiation pattern in the area near to the antenna is not equivalent to the pattern at large distances. The reactive near-field is a field pattern that surrounds an antenna element and, in this region, the electric and the magnetic field are very hard to predict. A short distance away from the reactive near-field, the radiating

near-field becomes dominant and it is the region where the radiation field of an antenna is taking its form. The field pattern at the large distances is refers to the term far field. The far field is the radiated power, also called the radiation field, and is what is most commonly of interest. Usually measurements and beam patterns are observed in the far-field region since it eases the calculations [2, 15].

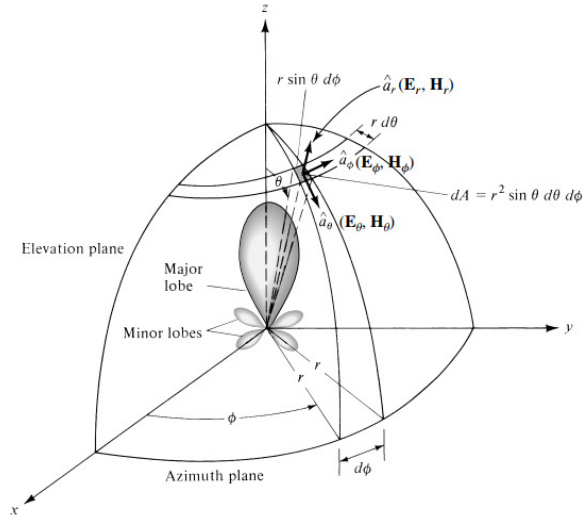


Figure 2.1: Spherical Coordinate Systems for Antenna Analysis [2]

2.1.2 Directivity

The directivity of an antenna is one of the most important parameters in this work, because antennas will be compared using this figure of merit. The directivity of an antenna has been defined by [2] as "the ratio of the radiation intensity in the provided guidance from the antenna to the radiation intensity averaged over all directions". Where the average radiation intensity, U_0 , is equivalent to the total power radiated by the antenna divided by

4π , which is the radiation intensity of an isotropic source. This can be expressed as:

$$D(\theta, \phi) = \frac{U(\theta, \phi)}{U_0} = 4\pi \frac{U(\theta, \phi)}{P_{rad}} \quad (2.1)$$

Where, D is the directivity of the antenna

U is the radiation intensity of the antenna

U_0 is the radiation intensity of an isotropic source

P_{rad} is the total power radiated

Since directivity is the ratio of two radiation intensities it is a dimensionless quantity. Hence, it is generally expressed in dBi. The directivity of an antenna permits to determine in which directions the antenna radiates with more or less intensity compared with an isotropic source. An antenna that has a narrow main lobe have better directivity, than the one which has a wide main lobe, henceforth it is more directive.

2.1.3 Gain

The gain is defined as "the ratio of the intensity, in a given direction, to the radiation intensity that would be obtained if the power accepted by the antenna were transmitted isotropically" [16]. It is noted that the definition is closely related to the directivity, as the difference between them is that the gain takes into account the conduction and dielectric efficiencies: The relationship between the antenna gain and directivity can be expressed by equation 2.2:

$$G(\theta, \phi) = 4\pi \frac{U(\theta, \phi)}{P_{in}} = 4\pi\eta \frac{U(\theta, \phi)}{P_{rad}} = \eta D(\theta, \phi) \quad (2.2)$$

Where, G is the gain of the antenna,

D is the directivity of the antenna.

P_{in} = total input power [W]

η = antenna efficiency ($0 \leq \eta \leq 1$)

2.1.4 Antenna Efficiency

Not all of the power transmitted to the feed of the antenna is radiated. Some of the power will be dissipated or reflected and thus, it is possible to define a number of efficiencies related to these losses: The reflection efficiency is related to the mismatch produced between the feeding line and the antenna when their impedance is different. The conduction efficiency is the ratio between the input power and the losses produced in the conductors of the antenna, and the same with the dielectric efficiency but taking into account the losses in the dielectric of the antenna instead of its conductors. Then, the total efficiency of an antenna is defined as follows,

$$e_0 = e_r e_c e_d \quad (2.3)$$

Where, e_0 = total efficiency

e_r = reflection (mismatch) efficiency

e_c = conduction efficiency

e_d = dielectric efficiency

Antenna's radiation efficiency is a multiplication of the conduction efficiency and the dielectric efficiency. The loss are due to: conduction and dielectric, this is called the I^2R losses.

2.1.5 Input Impedance

The input impedance of an antenna is characterized by [2] "the impedance presented by an antenna at its terminals or the proportion of the voltage to the current at both terminals

or the proportion of the proper components of the electric to magnetic fields at a point". It must be always taken into account when designing an antenna since it remarkably influences on the matching of an antenna. An appropriate impedance matching between a port and an antenna limits undesirable reflections. These two impedance's see each other as similar and it minimizes the reflection. Numerically input impedance is an aggregate of antenna's resistances and reactances at its terminals. Hence the impedance of the antenna can be written as in equation 2.4.

$$Z_{in} = R_{in} + X_{in} \quad (2.4)$$

Where, Z_{in} is the antenna impedance

R_{in} is the antenna resistance

X_{in} is the antenna reactance

The imaginary part, X_{in} of the input impedance which represents the power stored in the near field of the antenna. The resistive part, R_{in} of the input impedance comprises of two components, radiation resistance R_r and loss resistance R_L . The power associated with the radiation resistance is the power actually radiated by the antenna, while the power dissipated in the loss resistance is lost as heat in the antenna itself due to dielectric or conducting losses.

The input impedance depends on the geometry of conducting objects, their conductivity characteristics, the excitation method and characteristics of surrounding objects. Some antennas are not based on conducting metals and their resonance depends on, as an example, dielectric materials or slots in a plane. Their input impedance depend on other characteristics, such as the permittivity of the dielectric [2].

Impedance matching to minimize reflections is achieved by making the input impedance equal to the source impedance as given in the equation 2.5.

$$Z_{in} = Z_s^* \quad (2.5)$$

Where

$$Z_{in} = R_{in} + jX_{in}$$

$$Z_s = R_s + jX_s$$

Z_s is the source impedance

R_s is the source resistance

X_s is the source reactance

Maximum power transfer occurs when Z_{in} is the complex conjugate of Z_s . In other words, $R_{in} = R_s$ and $X_{in} = -X_s$. This is sometimes referred to as complex conjugate matching.

If the condition for matching is not satisfied then some of the power maybe reflected back, preventing all the power from reaching the destination point and this prompts to the creation of standing waves, which can be described by a parameter called as the Voltage Standing Wave Ratio (VSWR). VSWR is a "function of reflection coefficient" which is a measure of the reflected power from the antenna. When the reflection coefficient Γ is given, the value of VSWR is calculated using equation 2.6 [17]:

$$VSWR = \frac{1 + |\Gamma|}{1 - |\Gamma|} \quad (2.6)$$

$$\Gamma = \frac{V_r}{V_i} = \frac{Z_{in} - Z_s}{Z_{in} + Z_s} \quad (2.7)$$

Where, Γ is called the reflection coefficient

V_r is the amplitude of the reflected wave

V_i is the amplitude of the incident wave

The VSWR is basically a measure of the impedance mismatch between the transmitter and the antenna. The higher the VSWR, should not be more than 3, the greater is the mismatch. The minimum VSWR is unity, this represents a perfect match. In that situation, the power is not reflected from the antenna, which is ideal. Equation 2.9 shows the antenna with less VSWR, compared to the other antenna having higher VSWR, has better return loss. A practical antenna design should have an input impedance of either 50Ω or 75Ω since most radio equipment is built for this impedance.

2.1.6 Return Loss

It is a parameter that is used to measure the power reflected by the antenna due to the mismatch of the transmission line and antenna. Thus, the return loss is a parameter like the VSWR to demonstrate how well the matching between the transmitter and receiver has occurred. Its measurement describes the ratio of the reflected power in the reflected wave to the power in the incident wave in units of decibels [2, 18].

The Return Loss is given by:

$$ReturnLoss = -20\log|\Gamma|(dB) \quad (2.8)$$

Where $|\Gamma|$ represents the magnitude of the reflection coefficient and this value is always below 1.

For ideal matching between the transmitter and the receiver, $\Gamma = 0$ and $RL = -\infty$ which implies no power would be reflected back, whereas a $\Gamma = 1$ has a $RL = 0dB$, which implies that there is nothing to radiate by the antenna because the power provided to the antenna is completely reflected.

The Return Loss can also be calculated from the VSWR using the equation 2.9. Note that return loss is given as a ratio expressed in decibels.

$$ReturnLoss = -20\log\frac{VSWR - 1}{VSWR + 1}dB \quad (2.9)$$

The return loss is given as a negative figure. Being a loss the returned power must be less than the forward power, and hence the return loss has a minus sign or negative figures of decibels represent a loss.

2.1.7 S-parameters

The S-parameters are very important in microwave design for describing the behavior of electrical devices. Most of the electrical properties i.e. VSWR, return loss, gain and so on relates to the S parameters. S-parameters characterizes the input and output relationship between ports in an electrical system. The S-parameters S_{11} and S_{22} represent input and output reflection while S_{21} is the forward transmission coefficient (gain) and S_{12} are the reverse transmission coefficient (isolation) which measures the power transferred from port 1 to port 2. [19].

S_{11} (sometimes written as return loss) represents how much power is reflected from the antenna, and hence is known as the reflection coefficient. If $S_{11} = 0$ dB, then all the power is reflected from the antenna and nothing is radiated.

2.1.8 Bandwidth

The bandwidth of an antenna defined as the range of frequencies over which the performance of the antenna, with respect to specific characteristics, can operate correctly. The characteristics generally specified are gain, radiation pattern, the VSWR etc. Most

commonly, the VSWR is chosen as the parameter for bandwidth considerations and this bandwidth is known as the impedance bandwidth.

Bandwidth is the difference between the higher frequency (F_H) and lower frequency (F_L) for a particular band, as shown in equation 2.10.

$$BW = F_H - F_L \quad (2.10)$$

The bandwidth can also be described in terms of percentage of the center frequency of the band as:

$$BW = 100 \times \frac{F_H - F_L}{F_c} \quad (2.11)$$

Where, F_H is the highest frequency,

F_L is the lowest frequency, and

F_C is the center frequency in the band.

2.2 Types of Antennas

Antennas come in different shapes and sizes to suit different types of wireless applications. The qualities of an antenna are very much dictated by its shape, size and the type of material that it is made of. The antenna is the key component in mobile devices and plays an important role in the design of smart-phones. Antenna design for mobile phones wireless communication systems should have a small size, low cost, compact design and ability to operate in multiband which is usually a challenge. This section initiates the analysis of different antennas used in this work, which will be described below.

2.2.1 Printed Dipole Antenna

Printed dipole antennas are simple in structure, low cost, ease of fabrication, have a wide bandwidth with stable gain, and potential for high-efficiency operation. In light of these points of interest, printed dipole antennas have picked up interest for millimeter-wave phased array applications [20, 21]. The antenna consists of a 50Ω microstrip-line feed, a truncated ground plane, an integrated balun, and a printed dipole as shown in Figure 2.2.

The dipole and the ground plane are on the bottom layer of the substrate but the feedline is on the top layer. The dipole is fed by a slot line. For feeding purpose of the half wave dipole antenna there is a gap between two arms.

In this case, L is total length of the antenna, D is thickness of antenna arm and g is the feeding gap [12]. It is designed to operate from 26 to 30 GHz.

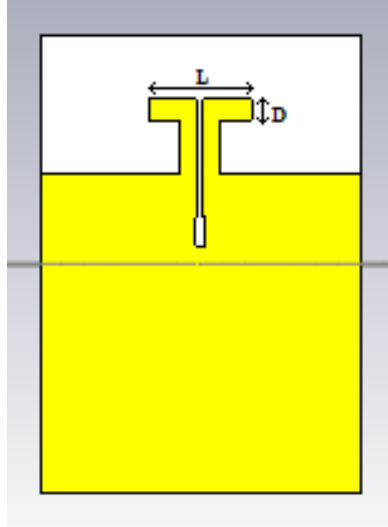


Figure 2.2: Structure of Printed Dipole Antenna

Printed antenna owing to variety of beneficial properties. These advantages include:

- They have better band width
- They are light weight, and low profile
- They occupy less area and volume
- They are low cost and ease of fabrication

In spite of its numerous advantages a printed dipole antenna suffers from the inherent disadvantage of incompatibility with wide band operation [22, 23, 24].

2.2.2 Microstrip Patch Antenna

The microstrip patch antenna consists of a metallic patch bonded to an insulating dielectric substrate, with a continuous metal layer bonded to the opposite side of the substrate which forms a ground plane as shown in Figure 2.3. The conducting patch can be rectangular, triangular, elliptical, circular or any other shape [25]. But rectangular shape is

used in this configurations, other configurations are complex to analyze and require heavy numerical computations. A microstrip patch antenna is characterized by its width, length, input impedance, radiation patterns and gain [26]. When designing a rectangular patch, the

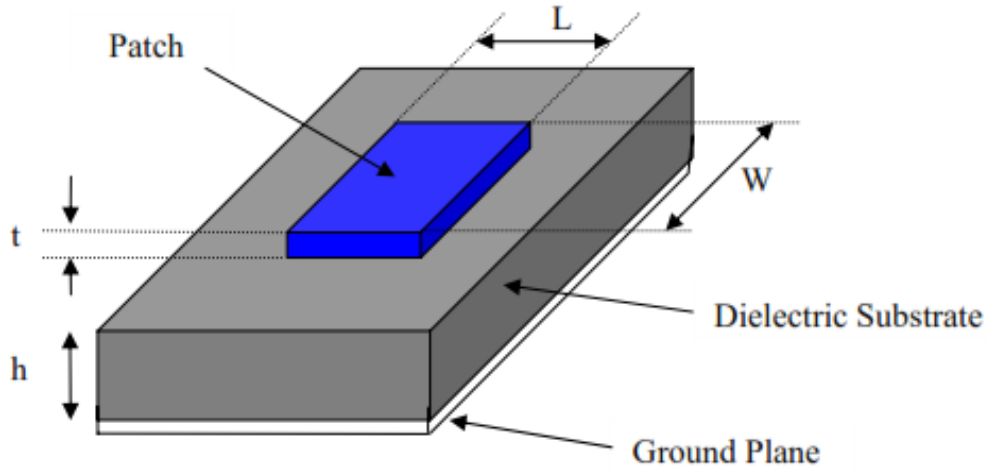


Figure 2.3: Structure of Microstrip Patch Antenna [3]

length L of the patch is usually $\lambda_0/3 < L < \lambda_0/2$, where λ_0 is the free-space wavelength. The patch is chosen to be very thin such that $t \ll \lambda_0$ (where t is the patch thickness). The height h of the dielectric substrate is usually $0.003 \lambda_0 \leq h \leq 0.05 \lambda_0$. For the design of microstrip patch antennas various substrates can be used. The value of the relative permeability (ϵ_r) relies upon the materials which can be aluminum, copper, gold or silver. The dielectric constant of the substrate is typically in the range $2.2 \leq \epsilon_r \leq 12$ is used [2, 27, 28].

Microstrip patch antennas have a tremendous commercial interest because of their numerous advantages. These advantages, as discussed in [2, 29, 30], include:

It is light weight, low profile, small volume.

It is low fabrication cost, ease of fabrication and conformity.

It is capable of dual and triple frequency operation.

It is compatible and easier to integrate with other micro strip circuits.

It can be realized in a very compact form, desirable for personal and mobile communication hand held devices.

These advantages that make microstrip patch antennas highly suitable for commercial mobile, high-speed communication applications also make them ideal for the aperstructure and opportunistic array concepts.

Microstrip patch antennas also have limitations. These are:

Narrow bandwidth

Lower power gain, poor radiation efficiency

Excitation of surface waves

Difficulty in achieving polarization purity

Lower power handling capability

The patch can be fed by means of a number of techniques and factors to be considered when designing a patch antenna are required for great performance. The dominant features of a micro strip array are controlled by substrate parameters such as thickness and permittivity more than by the particular element type. Because weight is a primary consideration in cellular system, a substrate must be chosen which has satisfactory dielectric properties, however which likewise has low density [31]. For good antenna performance, it is attractive to use a thick dielectric substrate having a low dielectric constant since this provides better efficiency, radiation and larger bandwidth however it requires larger element size [2, 32].

2.2.2.1 Feed Techniques

Microstrip patch antennas can be fed by a variety of methods. The four most commonly used feed techniques for microstrip patch antennas are the microstrip line, coaxial probe, aperture coupling and proximity coupling. These methods can be categorized into two: contacting and non-contacting. In the contacting method, the radio frequency power is fed directly to the radiating patch using a connecting element, for example, microstrip line and coaxial probe. In the non-contacting technique, electromagnetic field coupling is done to transfer power between the radiating patch and the microstrip line such as aperture coupling and proximity coupling [2, 19]. The most important thing to take note, regarding the maximum transfer of power, is the feed line should match with the input impedance of the antenna.

A) Microstrip transmission-line feed

The microstrip feed is more commonly used because it is very simple to design and easy to manufacture. The reason for the inset cut in the patch is to match the impedance of the feed line to the patch without the requirement of any additional matching element. This is accomplished by appropriately controlling the inset position. It is connected to the patch and the microstrip feed have smaller width compared with the width of the patch. Figure 2.4 shows microstrip patch antenna with microstrip transmission-line feed; the transmission line and the patch are made of the same material. Also, this type of feeding is mostly used in the case of patch array. The drawback is that one must make a compromise with the thickness and dielectric constant of the substrate. The surface waves and spurious feed radiation increases as the thickness of the dielectric substrate increases, this also increases the bandwidth of the antenna [2].

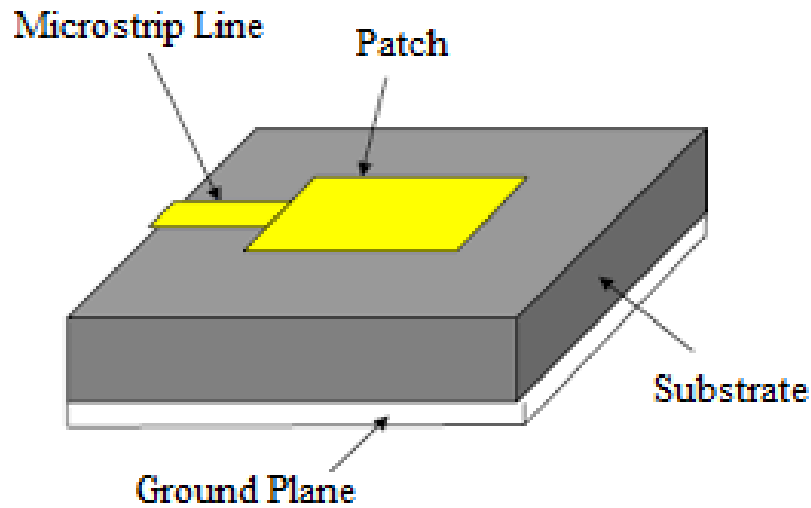


Figure 2.4: Microstrip Line Feed [3]

B) Coaxial probe feed

A hole is drilled through the substrate where the inner conductor of the coaxial connector extends through the dielectric and is soldered to the radiating patch, whereas outer core is connected to the ground plane. Figure 2.5 shows a microstrip antenna with coaxial feeding [33]. The main advantage of this method of feeding technique is that the feed can be placed at any desired location within the patch in order to match with its input impedance. The coaxial feed strategy is easy to manufacture and has low spurious radiation. However, a significant detriment is that it gives narrow bandwidth and is difficult to model since a hole has to be drilled in the substrate and the connector distends outside the ground plane [2, 33, 34].

C) Aperture coupling feed

In this sort of feed method, the radiating patch and the microstrip feed line are isolated by the ground plan as shown in the Figure 2.6. Coupling between the patch and the feed

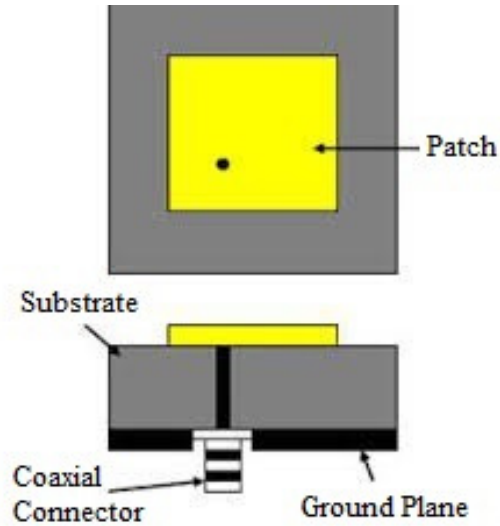


Figure 2.5: Coaxial Feed [3]

line is made with the help of a slot or an aperture in the ground plane. To improve the distinct electrical functions of radiation and circuitry, the thickness and dielectric constants of these two substrates can be chosen independently. The upper substrate is normally made with a lower permittivity to create loosely bound fringing fields, yielding better radiation. The lower substrate can be independently made with a high value of permittivity for tightly coupled fields that don't create deceptive radiation. The major disadvantage of this feed technique is that it is difficult to manufacture because of numerous layers, additionally it increases the antenna thickness. This feeding scheme also gives narrow bandwidth [2, 33].

D) Proximity coupling feed

This type of feed technique is also called as the electromagnetic coupling scheme. As shown in Figure 2.7, two dielectric substrates, with permittivity's ϵ_{r1} and ϵ_{r2} , are used such that the feed line is between the two substrates and the radiating patch is on top of the upper substrate. The fundamental advantage of this feed technique is that it disposes

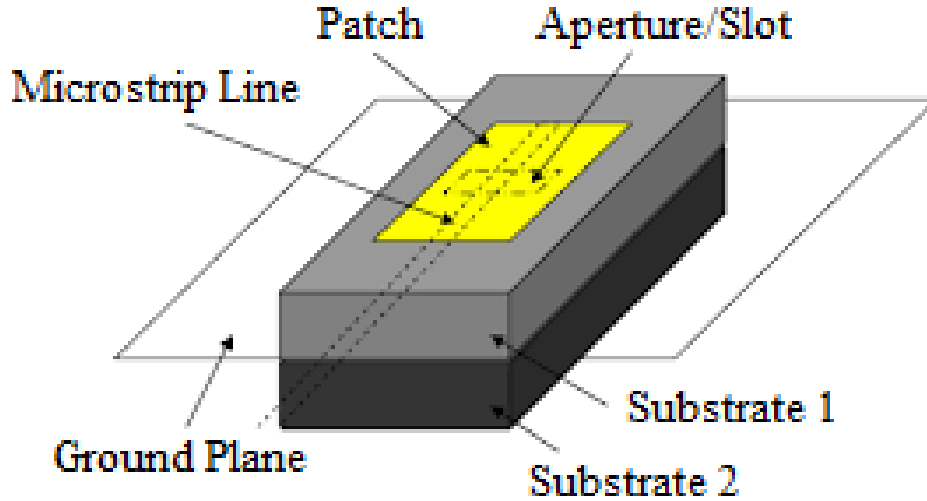


Figure 2.6: Aperture Coupled Feed [3]

spurious feed radiation and provides very high bandwidth [2], due to overall increase in the thickness of the microstrip patch antenna. To optimize the individual performances this scheme gives choices between two different dielectric media, which are for the patch and for the feed line. By controlling the length of the feed line and the width-to-line ratio of the patch matching can be accomplished. The significant disadvantage of this feed scheme is that it is difficult to fabricate because of the two dielectric layers which need proper alignment. Also, there is an increase in the overall thickness of the antenna.

2.2.3 Planar Inverted-F Antenna (PIFA)

PIFA has appeared as one of the most pledged candidates in the category of low profile antennas and is widely used for mobile communication [35, 36]. The proposed planar inverted-F antenna as shown in Figure 2.8 consists of the radiating patch, shorting plate and ground plane. The material used for the radiating element is copper. The dimension of the radiating patch is L_1 and L_2 and the ground plane is $L_g \times W_g$. The PIFA is at a height

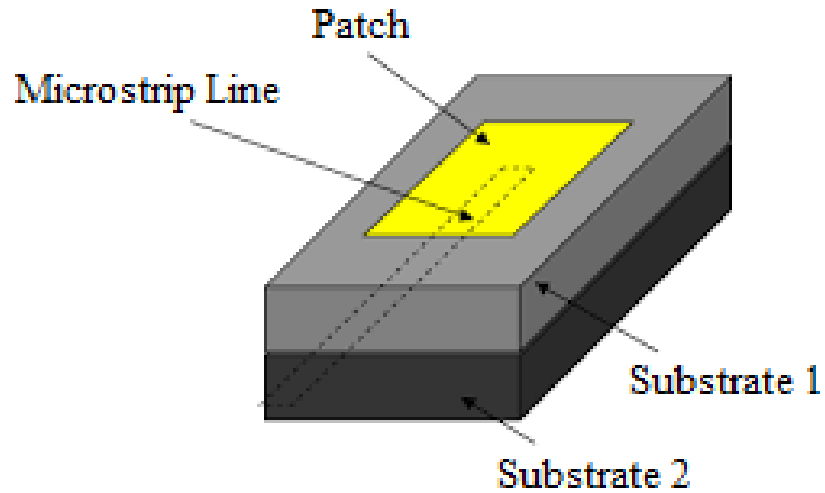


Figure 2.7: Proximity Coupling Feed [3]

h from the ground plane. The gap between the patch and the ground plane, h is filled with air substrate with permittivity, $\epsilon = 1$. The shorting plate is used to connect the antenna patch and ground plane. The distance of the feeding probe from the shorting plate is D whereas the shorting strip of the antenna has a width of W, and begins at one edge of the PIFA. In the simulation, the 50Ω discrete ports are used to feed in the bottom line of the rectangular patch.

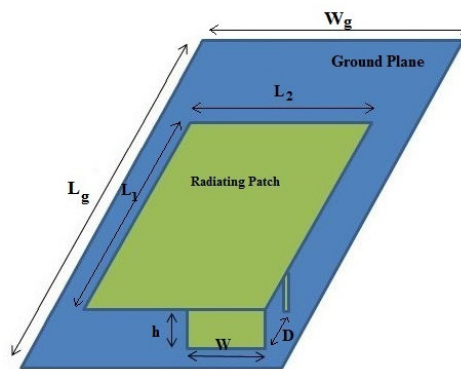


Figure 2.8: Structure of PIFA [4]

Planar Inverted-F Antenna (PIFA) have become popular for handheld wireless devices because of their many advantages such as [37, 38, 39].

Low profile, light weight, and small size

Simple design, low manufacturing cost, and ease of fabrication

Good radiation characteristics and good gain

Compact structure and being integrated with other handset components

Covering almost all frequency bands of the wireless services and applications

Apart from various advantages, PIFA structures also face limitations. Narrow bandwidth characteristic of PIFA is one of the major limitations for its commercial application in mobile phones. In addition to this, there is antennas vulnerability to physical damage, and directivity and input impedance are highly sensitive from the tradeoff point of view.

CHAPTER III DESIGN AND ANALYSIS

In this chapter design and analyze of the three different types of antennas is shown.

3.1 Designing of Printed Dipole Antenna

A general construction of a printed dipole antenna is shown in Figure 3.1. A Rogers RT/Duroid 5880 substrate is used for the printed dipole antenna design because it has low relative permittivity and most commonly used for mobile communication. The Rogers RT/Duroid 5880 substrate has a dielectric constant of $\epsilon_r = 2.2$, and loss tangent of $\tan\delta = 0.0009$ is utilized for the antenna design.

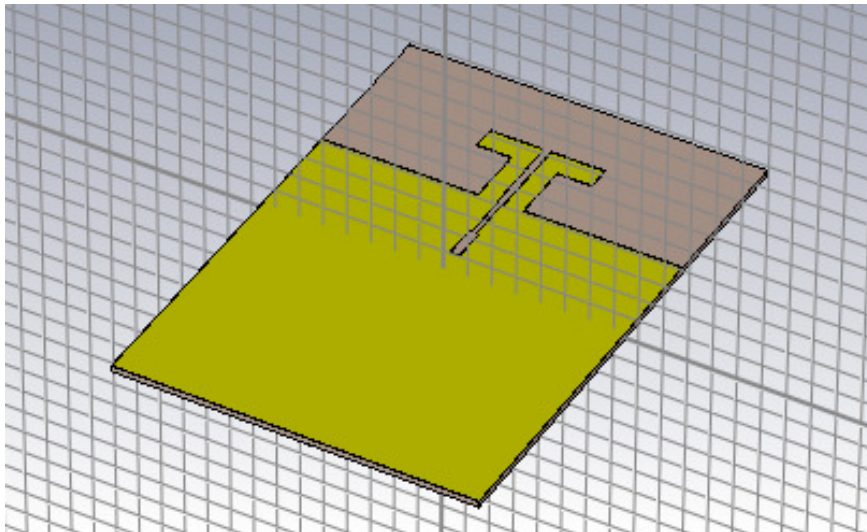


Figure 3.1: Designed single printed dipole antenna on CST MWS

The antenna is simulated with the help of CST MWS high-frequency structure simulator. Dimension of an antenna changes based on the resonant frequency. As a resonant frequency,

28 GHz has been chosen. Based on the operating frequency the optimized design parameters of the single element printed dipole antenna involves various calculations as follows [21]:

Calculation of operating wavelength λ_0

$$\lambda_0 = \frac{c}{f_r} \quad (3.1)$$

$$\lambda_0 = \frac{3 \times 10^8}{28 \times 10^9} = 10.714mm$$

Calculation of height of a substrate h

$$h \leq \frac{0.3 \times c}{2\pi \times f_r \sqrt{\epsilon_r + 1}} \quad (3.2)$$

$$h \leq \frac{0.3 \times 3 \times 10^8}{2\pi \times 28 \times 10^9 \sqrt{2.2 + 1}} \leq 0.285mm$$

Where, f_r is the resonant frequency,

c is the speed of light in free space.

ϵ_r is dielectric constant of substrate, which is 2.2

Thus lets take $h = 0.254$ mm

Calculation of length of the dipole

The length of the dipole is slightly less than half of the wavelength, because slightly reducing the length the antenna can become resonant. The antenna is said to be resonant when it is slightly less than a half-wave in length due to the end effect. End effect is due to a decrease in inductance and an increase in capacitance near the end of the conductor, which effectively lengthens the antenna. End effect increases with frequency and varies with different installations. Thus,

$$L = 0.45 \times \lambda_0 \quad (3.3)$$

$$L = 0.45 \times 10.714 = 4.8mm$$

The above resonant length (0.45 of wavelength) is valid if the dipole is very thin.

The thickness or width of arm of the dipole antenna, D is written as:

$$D = L/3 \quad (3.4)$$

$$D = 4.8/3 = 1.6mm.$$

For printed dipole array antenna, a high-gain series-fed printed dipole array antenna is proposed. The series-fed dipole array is a well known technique for increasing the gain of the antenna [35]. Each dipole has the same size, the spacing between each dipole is identical, and the dipoles are connected in series with a coplanar stripline. Number of elements in an array are four elements for observing the simulation results, they produce broadside radiation.

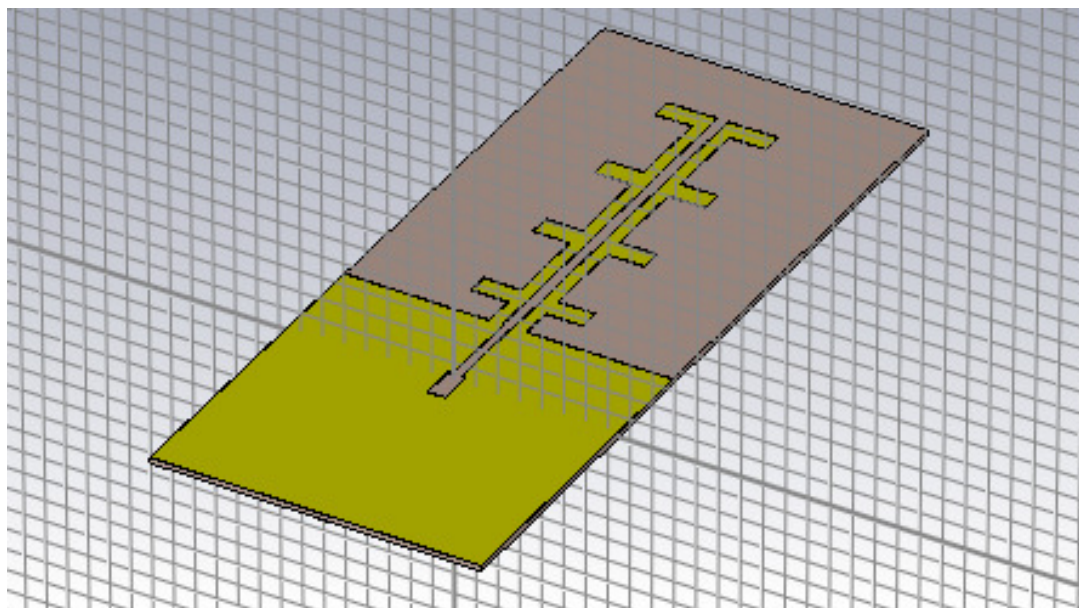


Figure 3.2: Designed printed dipole array antenna on CST MWS

Figure 3.2 illustrates the geometry of an four-element printed dipole array antenna, which is based on a single printed dipole antenna. Its element separation is 0.5 wavelengths. The length, spacing between, and width of each dipole were identical to those used in the single printed dipole antenna.

3.2 Designing of Microstrip Patch Antenna

To design a rectangular microstrip patch antenna the essential parameters are operating frequency of the antenna (f_r), the relative dielectric constant of substrate (ϵ_r) and thickness of the dielectric substrate (h). The choosing of these design parameters is important because the dimensions of a rectangular microstrip patch antenna and antenna performance depends on these parameters.

To have a big data rate for 5G mobile communication, the resonant frequency selected for the design is 28 GHz. The dielectric material selected for the design is RT5880 (lossy) which has a dielectric constant of 2.2. For the microstrip patch antenna to be utilized in mobile phones, it is essential that the antenna is not massive. Hence, the height of the dielectric substrate is selected as 0.15 mm.

The Performance of the microstrip antenna depends on its dimension. The radiation efficiency, return loss, gain, directivity and other related parameters are affected depending on the dimension of the patch. For an efficient radiation, the practical width of the patch can be calculated as [27, 40].

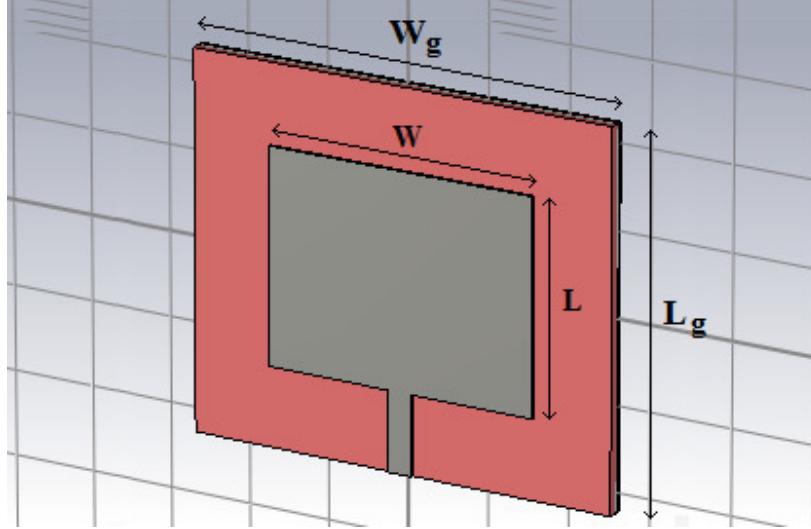


Figure 3.3: Designed single element microstrip Antenna

The Patch Width (W):

The practical width of the patch used is calculated using equation 3.5 [2].

$$W = \frac{c}{2f_0 \sqrt{\frac{(\epsilon_r + 1)}{2}}} \quad (3.5)$$

Where, c is speed of light, which is equal to 3×10^8 m/s,

ϵ_r is the relative dielectric constant of substrate

f_o is the operating frequency in Hz

W is the width of the patch element

Once we have $c = 3 \times 10^8$ m/s, $\epsilon_r = 2.2$ and $f_o = 28$ GHz, The corresponding value of the width becomes:

$$W = \frac{3 \times 10^8}{2 \times 28 \times 10^9 \sqrt{\frac{(2.2+1)}{2}}} = 4.235 \text{ mm}$$

The Effective Dielectric Constant (ϵ_{reff}):

Equation 3.6 is used to determine the effective dielectric constant of the microstrip patch antenna.

$$\epsilon_{reff} = \frac{\epsilon_r + 1}{2} + \frac{\epsilon_r - 1}{2} \left[1 + 12 \frac{h}{W} \right]^{-\frac{1}{2}} \quad (3.6)$$

$$\epsilon_{reff} = \frac{2.2 + 1}{2} + \frac{2.2 - 1}{2} \left[1 + 12 \frac{0.15}{4.235} \right]^{-\frac{1}{2}} = 2.1$$

Here, ϵ_{reff} is the effective dielectric constant and h is the height of dielectric substrate.

The Effective Length (L_{eff}):

The length of the patch looks electrically slightly larger than the usual length of design, because of the fringing field along the patch width, and this parameter can be calculated by using equation 3.7:

$$L_{eff} = \frac{c}{2f_0 \sqrt{\epsilon_{reff}}} \quad (3.7)$$

Substituting the values $c = 3 \times 10^8$ m, $f = 28 \times 10^9$ GHz and $\epsilon_{reff} = 2.1$,

We get:

$$L_{eff} = \frac{3 \times 10^8}{2 \times 28 \times 10^9 \sqrt{2.1}} = 3.69mm$$

Calculation of the length extension (ΔL):

Due to the fringing fields along the antenna it is appropriate to use extended length for a better performance. The length is extended by (ΔL) given by the equation 3.8.

$$\Delta L = 0.412h \frac{\epsilon_{eff} + 3\left(\frac{w}{h} + 0.264\right)}{\epsilon_{eff} - 0.258\left(\frac{w}{h} + 0.8\right)} \quad (3.8)$$

Obtaining $\varepsilon_{reff} = 2.1$ mm, $W = 4.235$ mm and $h = 0.15$ mm, then the length extension becomes:

$$\Delta L = 0.412 \times 0.15 \frac{2.1 + 3 \times \left(\frac{3.29}{0.15} + 0.264\right)}{2.1 - 0.258\left(\frac{3.29}{0.15} + 0.8\right)} = 0.077$$

Calculation of actual length of patch (L):

After the calculation of each of effective and extended lengths of the patch, the actual value of the radiating patch length (L) is calculated by using equation 3.9.

$$L = L_{eff} - 2\Delta L \tag{3.9}$$

$$L = 3.69mm - 2 \times 0.077mm = 3.536mm$$

The patch thickness, t is chosen to be very thin such that $t \ll \lambda_0$ and for this case it is selected at $t = 0.035$ mm which is one of the standard thickness dimension at mmwave frequency.

Calculation of the ground plane dimensions (L_g and W_g):

The transmission line model is applicable to infinite ground planes only. However, for practical considerations, it is basic to have a finite ground plane. It is shown by [34] that comparable outcomes for finite and infinite ground plane can be acquired if the size of the ground plane is greater than the patch dimensions by approximately six times the substrate thickness all around the periphery. Hence, for this structure, the ground plane measurements would be given as:

$$L_g = 6h + L \tag{3.10}$$

$$L_g = 6(0.15) + 3.536 = 4.436mm$$

$$W_g = 6h + W \tag{3.11}$$

$$W_g = 6(0.15) + 4.235 = 5.135mm$$

Where, L_g and W_g are the length and width of the ground plane, h is the height of the substrate, L and W are the length and width of the patch element respectively.

Equations 3.10 and 3.11 are used to determine the dimension of the ground plane, there's no need for the calculation of the dimension of the substrate because their dimensions are similar with that of the ground plane. i.e. $L_s = L_g = 6h + L$ and $W_s = W_g = 6h + W$. Where, L_s and W_s are the length and width of the substrate.

After determining the dimensions of the rectangular patch, one should consider the feeder type. Here, microstrip line method with corporate-feed network model is chosen as a feeding technique since it is easy to fabricate and control the feeding position.

Design of 4x1 Patch Antenna Array

Antenna arrays are used to scan the beam of an antenna system, to increase the gain, directivity and upgrade different capacities which would be troublesome with single element antenna. For microstrip antenna array, microwave signal divider or feed network is often used to regulate the amplitude and phase feed requirements of the radiating elements (patches) to control the beam scanning properties. Elements can be fed by a single line or multiple lines in a feed network arrangement [2, 27]. Thus selecting, optimizing and implementing the feed network forms a critical part of the antenna array design. The most common and well-known feeding methods of the microstrip array antenna are:

Series feed network

Corporate feed network

I. Microstrip Series Feed Network:

A series feed arrangement of microstrip array is shaped by interconnecting all the patch elements in series with high impedance transmission line and the input power is feed at the first element. This is shown in Figure 3.4. It is more complex, although it uses up less space. Here two successive patch elements are matched with the help of quarter wavelength transformer method. In this class of feeder, as the wave travels through the microstrip line, it is attenuated because of power radiated from each element of the array [27]. **II.**

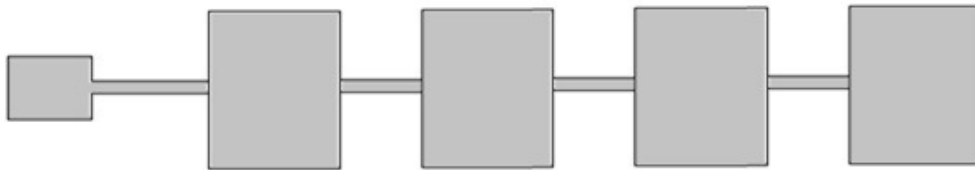


Figure 3.4: Microstrip series feed network [5]

Microstrip Corporate Feed Network

Corporate feed array is general, versatile and the most widely used configuration. This has a single input port and numerous feed lines in parallel which is terminated at an individual radiating component which could be a patch. This method has more control of the feed of every element and is perfect for scanning phased arrays, multi beam arrays. The distance between the patches and the microwave feed point of the array are kept equal for equal phase patch excitation. The incident power split is accomplished by using either tapered lines or using quarter wavelength impedance transformers [27, 41].

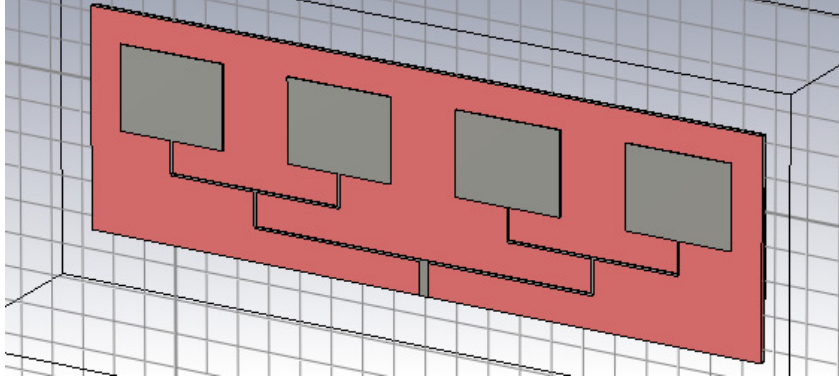


Figure 3.5: 4×1 corporate feed microstrip array antenna using CST model

In this thesis, as shown in the Figure 3.5, corporate feed network using the tapered lines method to match the individual sections to a 50Ω line source is used. The design consists of four microstrip patches with an equal spacing of $\lambda/2$.

3.3 Designing of Planar Inverted-F Antenna (PIFA)

The geometry of the single band PIFA element is shown in Figure 3.6 which is designed using CST studio suite. The design for this structure is based on Rogers RT5880 (lossy) substrate material with dielectric constant of 2.2.

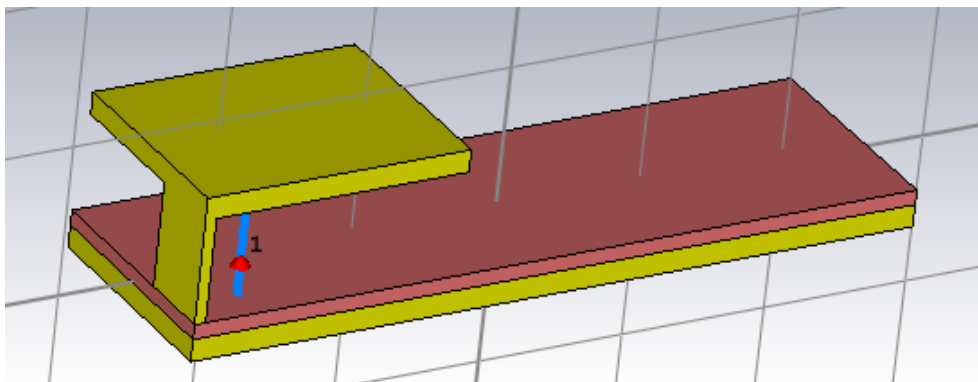


Figure 3.6: Designed single PIFA on CST MWS

The operating frequency of a PIFA antenna is inversely proportional to its physical dimensions. In designing the proposed antenna the length and width, L_1 and L_2 of the radiating patch can be calculated using formula as shown in equations 3.12 - 3.14. Equation 3.13 shows that the resonant frequency is inversely proportional to the radiating patch lengths as presented in [42]. The frequency of operation, f used in the calculation is 28 GHz.

$$L_1 + L_2 - W = \frac{\lambda}{4} \quad (3.12)$$

$$f_0 = \frac{c}{4(L_1 + L_2 - W)} \quad (3.13)$$

$$L_2 = \frac{c}{4f} \sqrt{\frac{2}{\epsilon_r + 1}} \quad (3.14)$$

Where, c is free space velocity of light, which is equal to 3×10^8 m/s, f is frequency of operation and L_1, L_2 and W is the width of radiating patch, length of radiating patch and width of the shorting plate, respectively.

Thus, the length of radiating patch becomes;

$$L_2 = \frac{c}{4f} \sqrt{\frac{2}{\epsilon_r + 1}} = \frac{3 \times 10^8}{4 \times 28 \times 10^9} \sqrt{\frac{2}{2.2 + 1}} = 1.8 \text{ mm}$$

Taking the value of the width of shorting plate 0.5 mm then the width of radiating patch is found from equation 3.12 as:

$$L_1 = \frac{\lambda}{4} - L_2 + W = 10.714/4 - 1.8 + 0.5 = 1.378 \text{ mm}$$

The patch length and width are optimized by several simulations to 1.8 mm and 1.4 mm, respectively. The height, h of top radiating patch from ground plane can be reduced to a great extent, which further results in reducing thickness of mobile phones. So, the height of

PIFA can be taken as small as 0.5 mm from equation 3.15 and the distance of the feeding position to the shorting plate is $d = 0.43$ mm.

$$h = \frac{0.0606\lambda}{\sqrt{\epsilon}} \quad (3.15)$$

$$h = \frac{0.0606 \times 10.714}{\sqrt{2.2}} = 0.5mm$$

The size of the ground plane, $L_g = L + 6 \times h = 5mm$ and $W_g = W + 6 \times h = 4mm$. The size of the substrate is also is 5 mm x 4 mm. The calculated value used as a preliminary dimensions of the patch. The above conditions, 3.12 to 3.14 demonstrated that the total of the radiating patch length and width must be quarter wavelength ($\lambda/4$).

The proposed PIFA array antenna is constructed by using four identical PIFA antenna elements as shown in Figure 3.7. The separation distance among antenna elements is chosen to be half-wavelength at the resonant frequency.

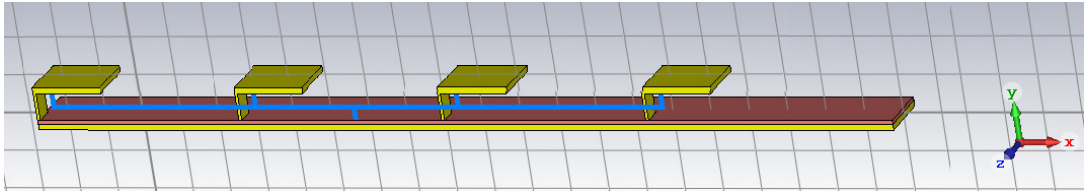


Figure 3.7: Geometrical configuration of four-element PIFA array antenna

CHAPTER IV

SIMULATION RESULTS

After all the necessary dimensions are calculated, the software used to model and simulate the proposed antennas is CST Studio Suite 2018's MWS. The software consists of several modules which are aimed to design different segments of components. CST MWS performs fast and accurate 3D EM simulation of high frequency applications. It provides shorter development cycles and enables virtual prototyping before physical trials. CST MWS will be used to calculate and plot the gain, return loss, VSWR, radiation pattern, directivity and efficiency. The operating frequency of all the designed antennas is about 28 GHz which is suitable for 5G mobile communication.

4.1 Simulation Result for Printed Dipole Antenna

The proposed printed dipole antenna of length 4.8 mm, width 1 mm and feed gap 0.3 mm is simulated and observed to resonate at 28 GHz frequency. The default units of the values for frequency GHz and for length mm, are selected. Global mesh properties have been optimized for making the simulation fast and more accurate.

S-parameters

After the simulation, S-parameter has been observed as in the Figure 4.1 and 4.2 for single element and array elements of printed dipole antenna, respectively.

From these figures it is found that the value of return loss at the center of frequency, 28 GHz, for single printed dipole antenna is -10.97 dB and for the printed dipole array antenna is -7.57 dB (approx.).

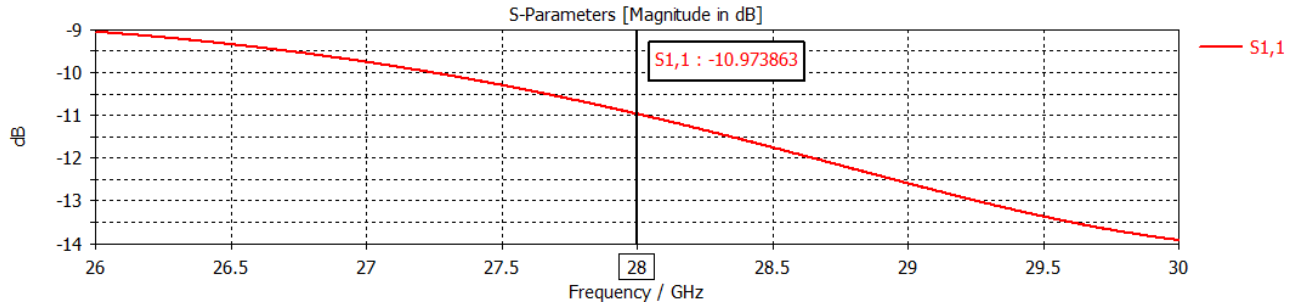


Figure 4.1: S-parameter for single printed dipole antenna

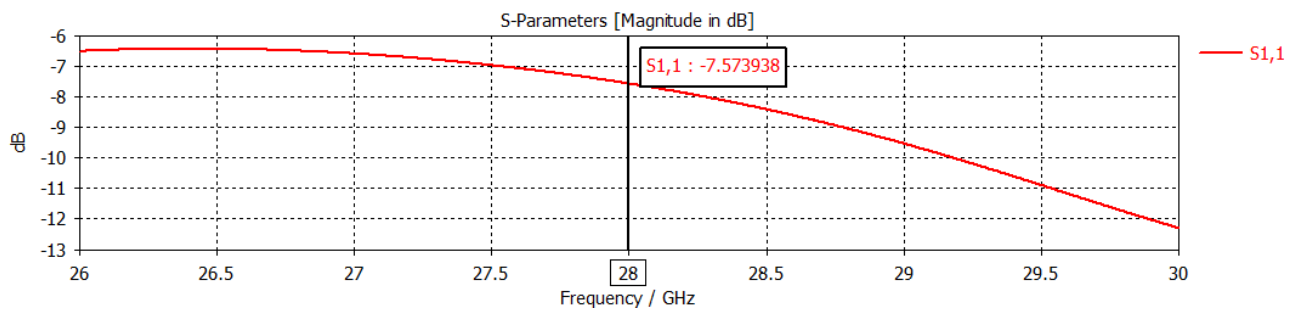


Figure 4.2: S-parameter for 4×1 printed dipole array antenna

VSWR

The value of VSWR at frequency of 28 GHz as can be seen from Figures 4.3 and 4.4 for single printed dipole antenna and for printed dipole array antenna, respectively, is equal to 1.78 and 2.4 (approx.).

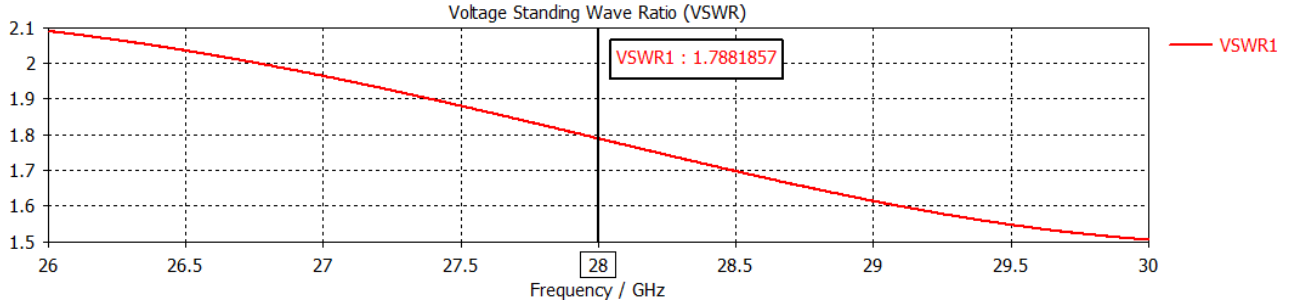


Figure 4.3: VSWR plot of single printed dipole antenna

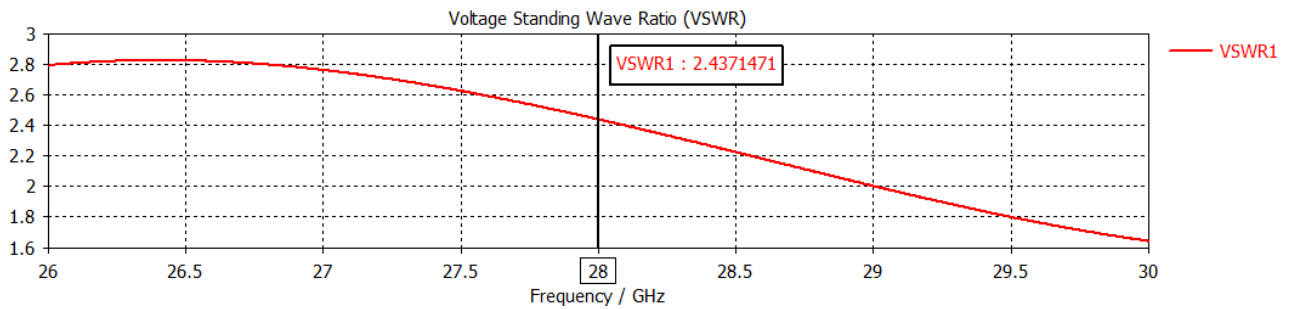


Figure 4.4: VSWR plot of 4x1 printed dipole array antenna

Radiation Pattern:

The three dimensional far-field radiation pattern views of the single and 4 × 1 printed dipole array antenna are shown from Figure 4.5 to 4.8. The gain and directivity, respectively, are found to be 5.06 dBi and 5.28 dBi for single printed dipole antenna, and 9.87 dBi and 10.12 dBi for printed dipole array antenna. Red color shows the maximum radiation while the blue color shows the minimum radiation. The power plot for the azimuthal angle is shown in Figure 4.9.

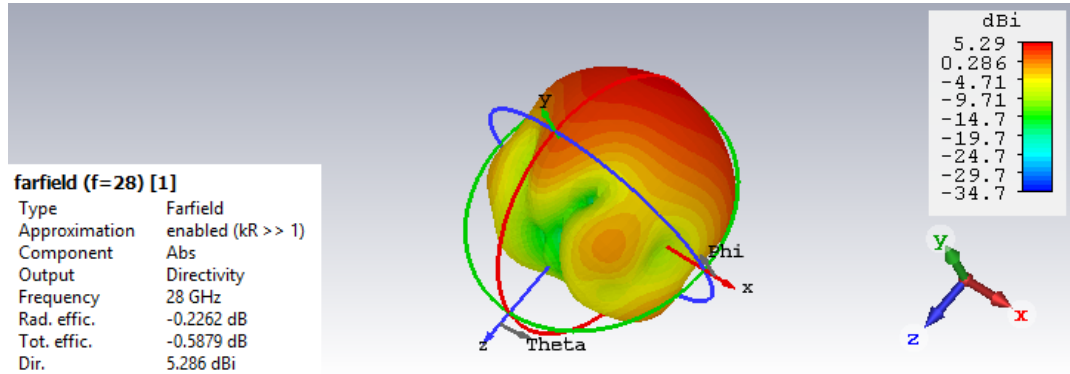


Figure 4.5: 3-D far-field radiation pattern of single printed dipole antenna

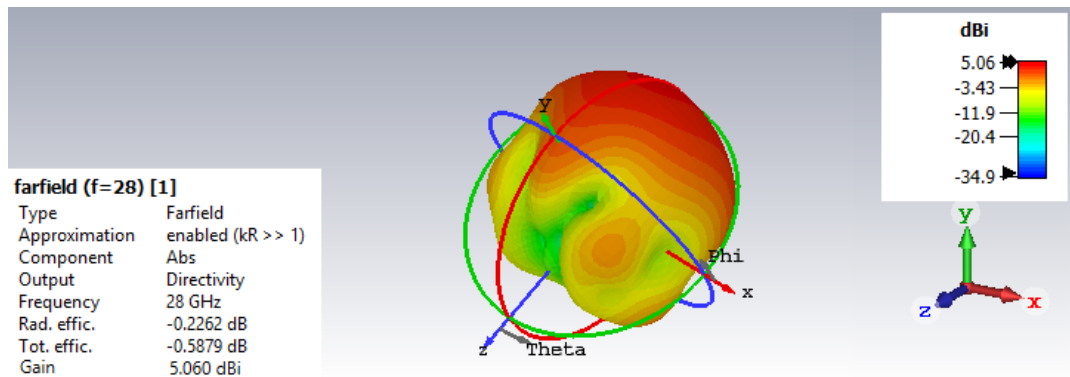


Figure 4.6: 3-D far-field gain of single printed dipole antenna

4.2 Simulation Result for Microstrip Patch Antenna

S-parameters

After the simulation, taking values of height of substrate $h = 0.15$ mm, width of the patch $W = 4.235$ mm and length of the patch $L = 3.536$ mm, S-parameter of single and array of microstrip patch antenna are observed as in Figure 4.10 and 4.11, respectively.

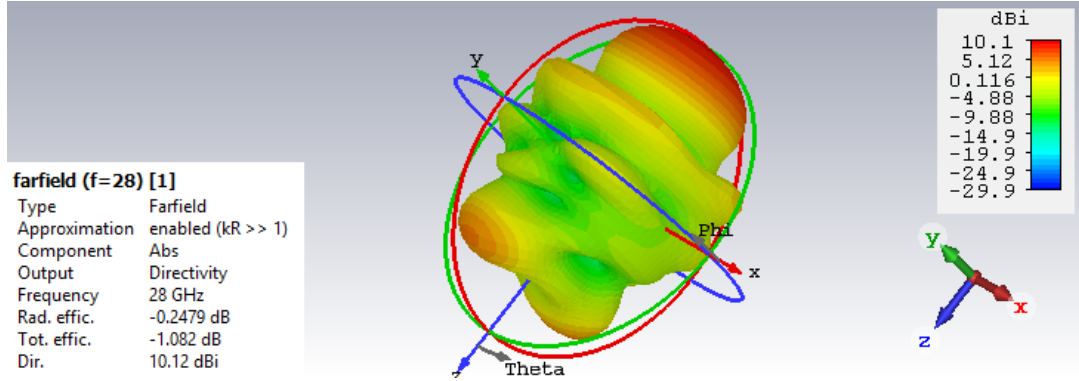


Figure 4.7: 3-D far-field radiation pattern of 4×1 printed dipole array antenna

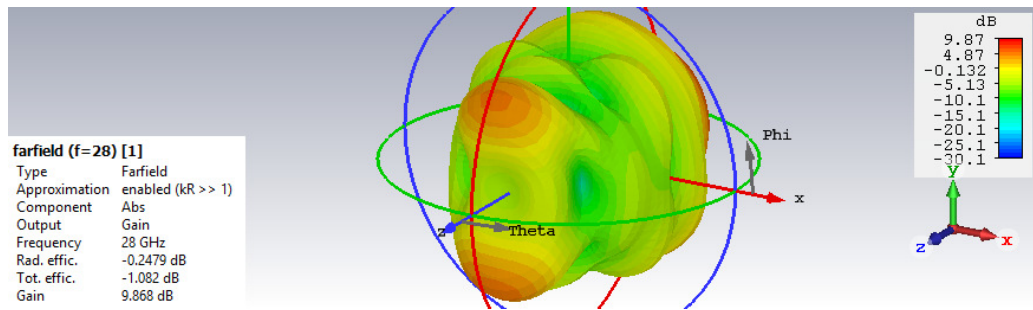


Figure 4.8: 3-D far-field gain of 4×1 printed dipole array antenna

From Figures 4.10 and 4.11 the value of return loss at resonating frequency of 28 GHz has been found as -9.27 dB for single microstrip patch antenna and -27.37 dB microstrip patch array antenna.

VSWR

Figure 4.12 and 4.13 which are captured from the simulated result of CST software shows VSWR for microstrip patch antenna at frequency of 28 GHz is equal to 2.05 for single element and 1.09 for 4×1 array elements.

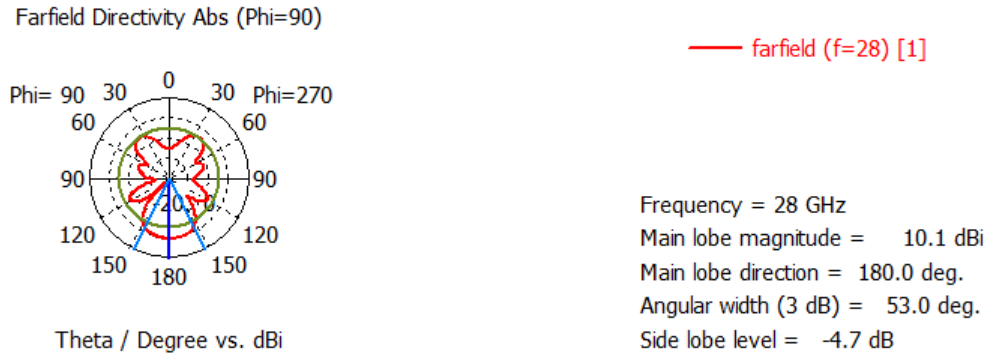


Figure 4.9: 3-D polar plot of 4×1 printed dipole array antenna

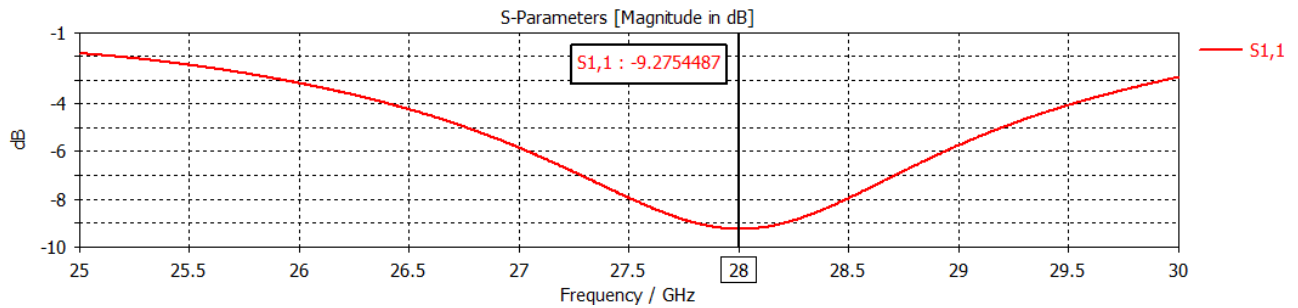


Figure 4.10: S-parameter for single microstrip patch antenna

Radiation Pattern Plots

A microstrip patch antenna radiates normal to its patch surface. Figure 4.14 shows the 3D radiation pattern of the single microstrip patch antenna at the designed frequency, and its gain is found as 5.94 dBi and directivity is found as 6.44 dBi. Figure 4.16 and 4.17 shows the 3D radiation pattern of the 4×1 microstrip patch array antenna, and its directivity and gain are found as 12.37 dBi and 12.09 dBi, respectively. The power plot is shown in Figure 4.18 for array of microstrip patch antennas.

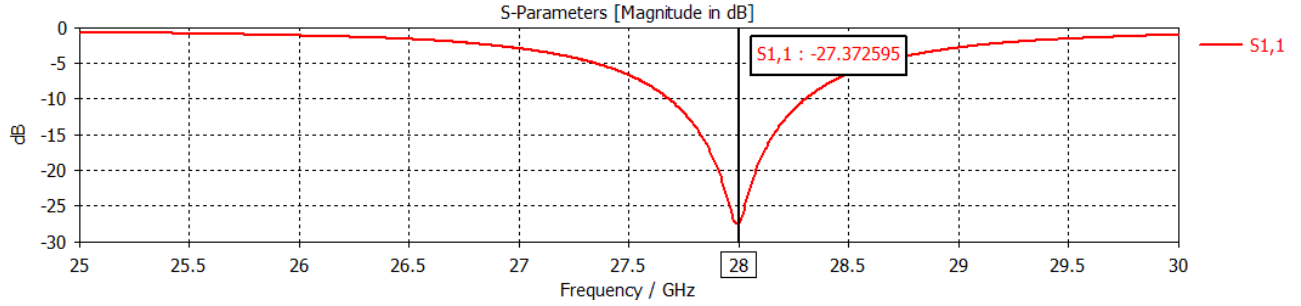


Figure 4.11: S-parameter for 4×1 microstrip patch array antenna

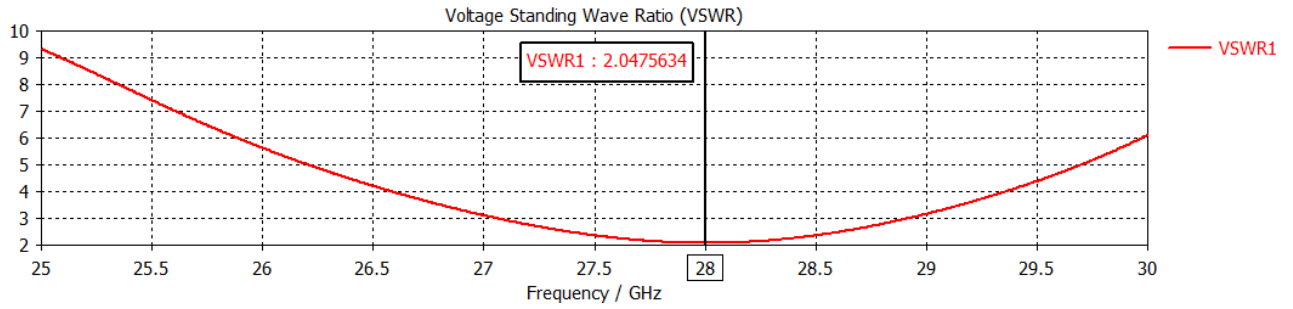


Figure 4.12: VSWR plot of single microstrip patch antenna

4.3 Simulation Result for Planar Inverted-F Antenna

S-parameters

The scattering parameter, S_{11} of the single PIFA and 4×1 planar inverted-F array antenna, respectively, is given in Figure 4.19 and 4.20. The value of return loss at 28 GHz for single and 4×1 elements of this antenna is found to be -1.6 dB and -2.5 dB (approx.).

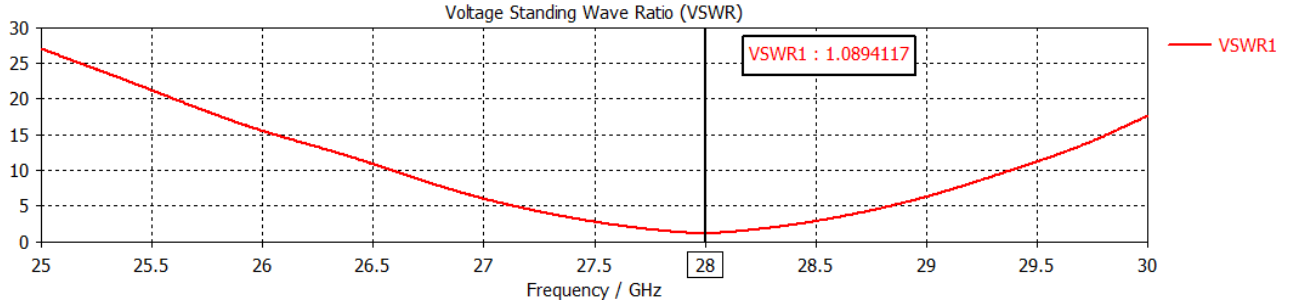


Figure 4.13: VSWR plot of 4×1 microstrip patch array antenna

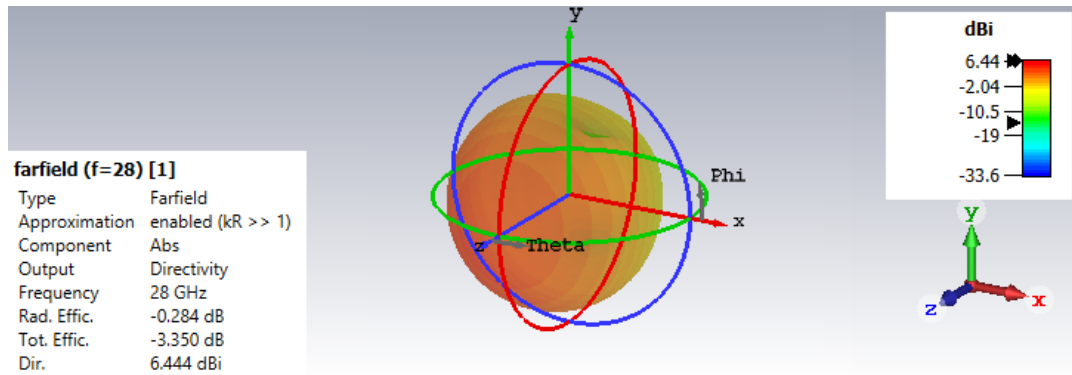


Figure 4.14: 3-D far-field radiation pattern of single microstrip patch antenna

VSWR

From the Figures 4.21 and 4.22 it can be observed that the VSWR of single PIFA is equal to 2.9 and that of PIFA array is equal to 2.6 (approx.) at 28 GHz.

Radiation Pattern:

The radiation pattern plot of PIFA antenna shows from Figures 4.23 to 4.26 which is obtained at the respective operating frequency. It is a plot of the antenna gain and directivity versus the elevation angle. The antenna has a gain of 2.9 dBi and directivity of

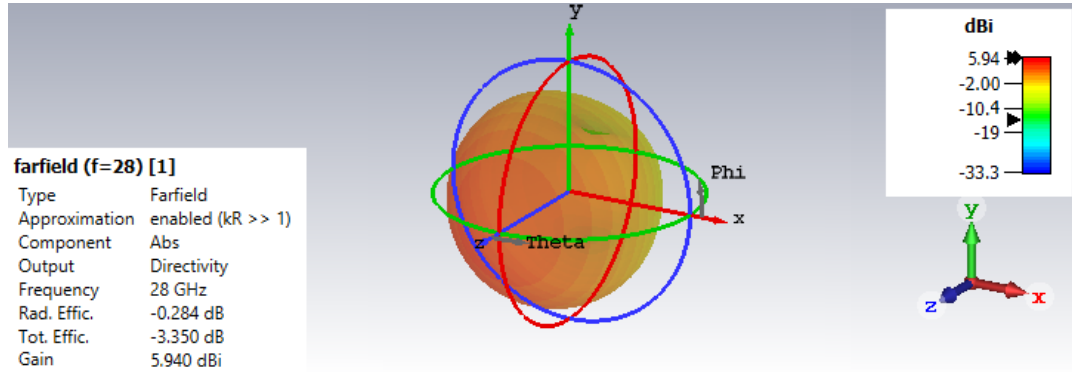


Figure 4.15: 3-D far-field gain of single microstrip patch antenna

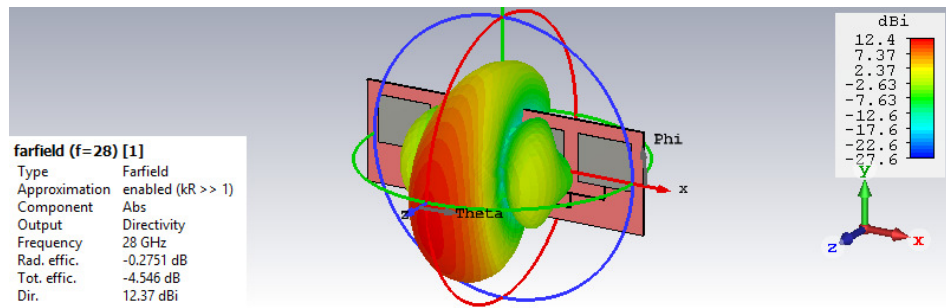


Figure 4.16: 3-D far-field radiation pattern of 4×1 microstrip patch array antenna

2.92 dBi for single PIFA, and gain of 9.79 dBi and directivity of 9.81 dBi for array PIFA at 28 GHz. Power plot for the azimuthal angle is shown in Figure 4.27.

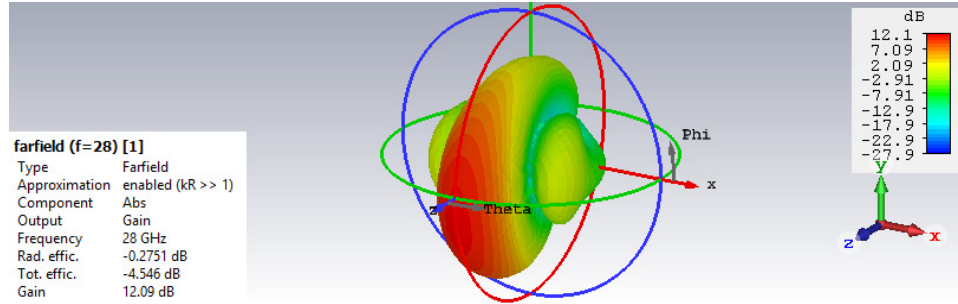


Figure 4.17: 3-D far-field gain of 4×1 microstrip patch array antenna

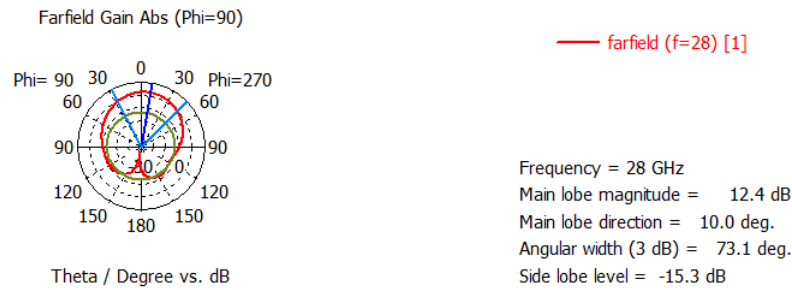


Figure 4.18: 3-D polar plot of 4×1 microstrip patch array antenna

The above results are summarized in Table 4.1, to easily observe which antenna has a better antenna performance.

From these three antennas microstrip patch antenna is selected as a good candidate for 5G mobile communication since it has a better gain, directivity, VSWR and return loss with relatively same efficiency. Next the performance of microstrip patch antenna is analyzed by changing the essential parameters such as dielectric constant of substrate (ϵ_r), the height of the dielectric substrate (h), the width of the patch (W), the length of the patch (L).

The analysis is based on the four scenarios of observation. In the first scenario the effect on the antenna characteristics by varying the substrate material of the patch, then in the

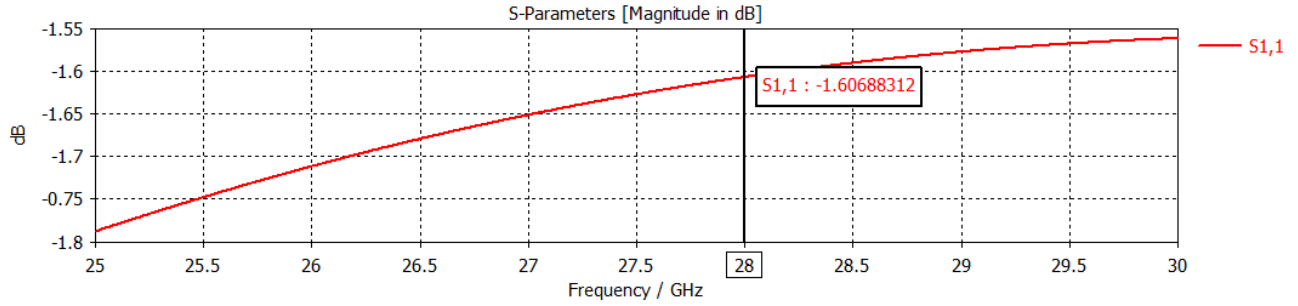


Figure 4.19: S-parameter for single PIFA antenna

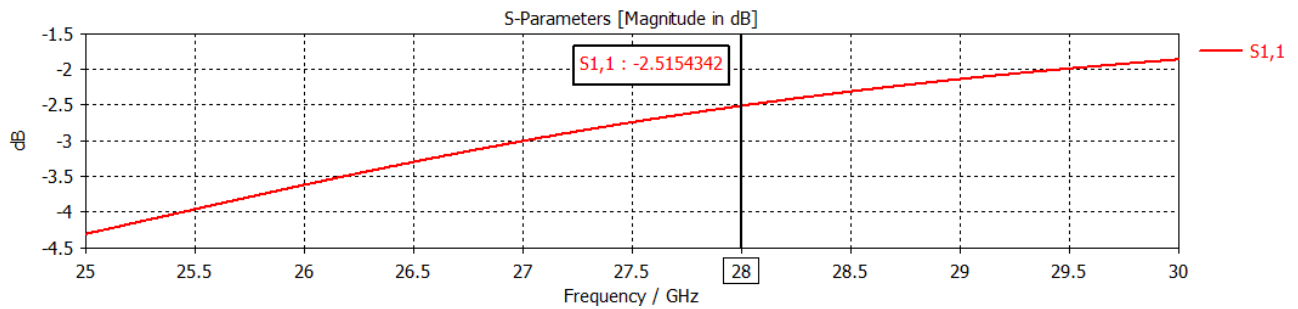


Figure 4.20: S-parameter for 4x1 PIFA array antenna

second and third scenarios it analyzes the effect on the antenna characteristics by varying the length of the patch and the width of the patch, respectively. In the last scenario the height of the substrate is varied to observe the variation in the antenna characteristics.

Effect of Changing Substrate Material

The material which has the dielectric constant in the range of $2.2 \leq \epsilon_r \leq 12$ can be used as substrate for microstrip patch antenna [1]. The system performance changes at the point when the thickness of substrate and the substrate material of a microstrip antenna are changed. In this way, in order to introduce appropriate accuracy in the design structure of the antenna, it is important to know the impact of changing dielectric substrate material.

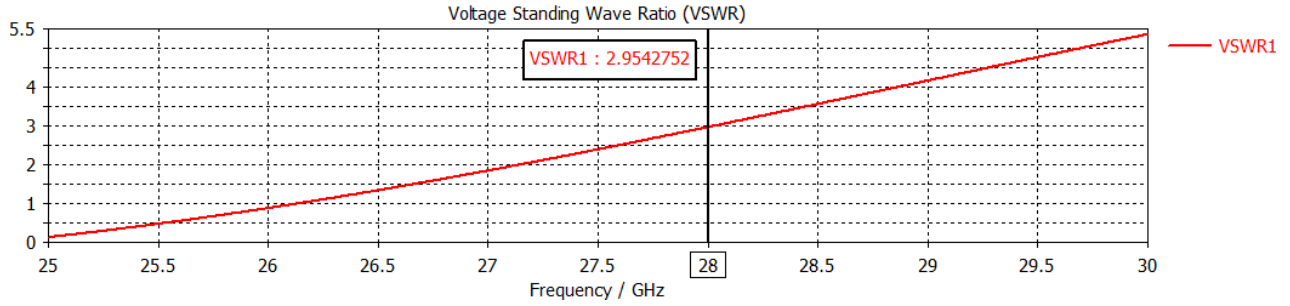


Figure 4.21: VSWR plot of single PIFA antenna

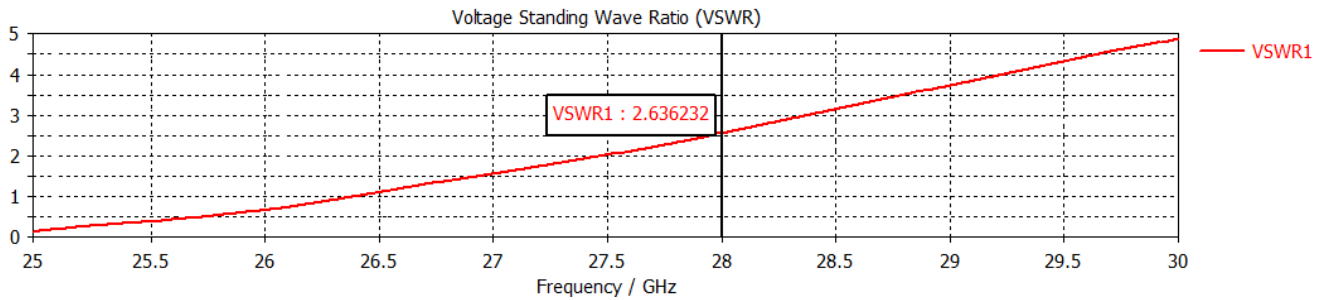


Figure 4.22: VSWR plot of 4x1 PIFA array antenna

With changing the substrate material, the dielectric constant (ϵ_r) of the substrate changes. Here, four different substrate materials such as Rogers RT5880, RO4725, RT6002, RO4350B, and RF-4 with dielectric constants 2.2, 2.64, 2.94, 3.66 and 4.3, respectively were tested to see the behavior of their performance. For every different substrate material, the antenna performance parameters are analyzed like gain, directivity, return loss, bandwidth and the dimensions of patch of the antenna (length of patch and width of patch), where the antenna configuration is same and the operating frequency is 28 GHz. These antennas are designed and simulated by using CST MWS simulator. i.e. the height of the substrates is fixed at 0.2 mm. Table 4.2 shows the summary of variation on antenna parameters with

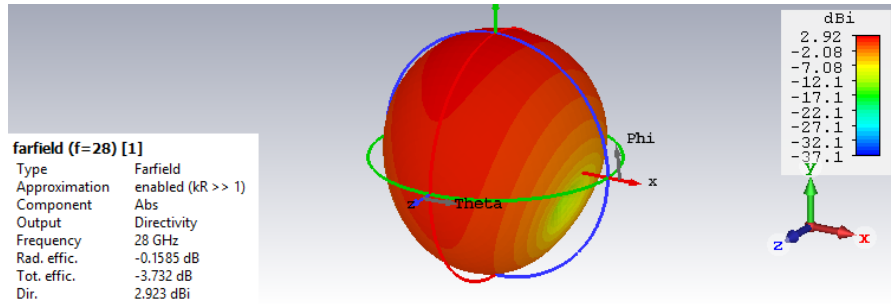


Figure 4.23: 3-D far-field radiation pattern of single PIFA

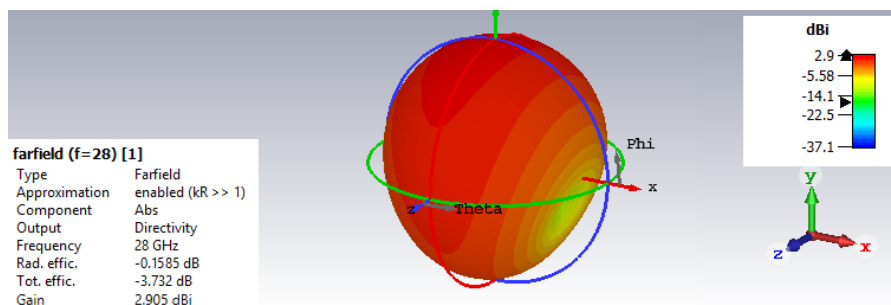


Figure 4.24: 3-D far-field gain of single PIFA

changing substrate material. NB: The height of the substrates is fixed at 0.2 mm, unlike the previous results of microstrip patch array antenna.

From the simulations, it is clearly shown in Table 4.2 that the higher the value of the dielectric constant, the lower the directivity and bandwidth but the patch antenna size become small since the length of patch (L) and width of patch (W) decreases. A maximum of 12.4 dBi directivity is obtained using Duroid RT5880 substrate material with a dielectric constant of 2.2, while a directivity of 11.47 dBi is obtained using FR-4 substrate material. The results prove that using a substrate material with a lower dielectric constant in design of microstrip patch antenna leads to better antenna performance.

Parameter	Printed Dipole Antenna		Microstrip Patch Antenna		PIFA	
	Single	Array	Single	Array	Single	Array
Gain (dBi)	5.06	9.87	5.94	12.09	2.9	9.79
Directivity (dBi)	5.28	10.12	6.44	12.37	2.92	9.81
Rad. efficiency (dB)	-0.226	-0.248	-0.284	-0.275	-0.15	-0.18
VSWR	1.78	2.4	2.05	1.09	2.9	2.6
Return Loss (dB)	-10.97	-7.57	-9.27	-27.37	-1.6	-2.5

Table 4.1: Comparison of antennas performance

Substrate Name	RT5880	RO4725	RT6002	RO4350B	FR-4
Dielectric constant (ϵ_r)	2.2	2.64	2.94	3.66	4.3
Length of patch (mm)	3.51	3.21	3.05	2.74	2.53
Width of patch (mm)	4.24	3.97	3.82	3.50	3.29
Gain (dBi)	12.18	11.52	11.46	10.70	10.34
Directivity (dBi)	12.4	12	11.76	11.49	11.47
Return Loss (dB)	-31.14	-23.47	-26.55	-40.31	-24.22
Bandwidth (GHz)	0.748	0.683	0.672	0.665	0.658

Table 4.2: Effect of substrate material

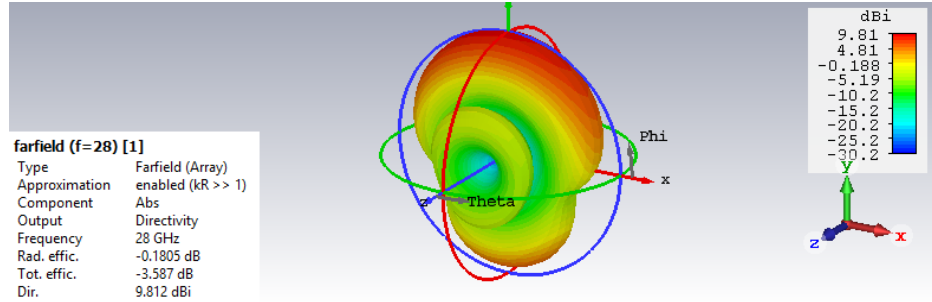


Figure 4.25: 3-D far-field radiation pattern of 4×1 PIFA array antenna

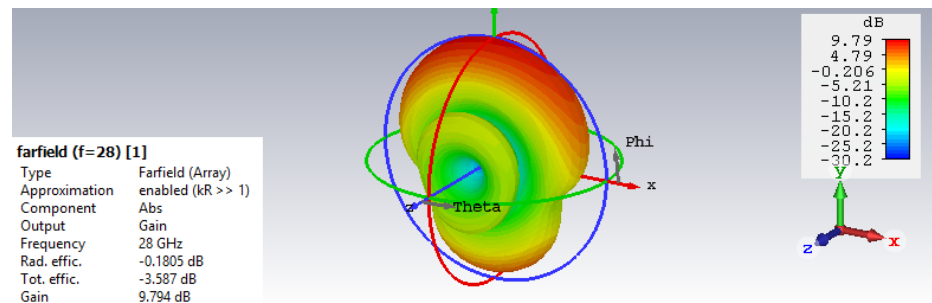


Figure 4.26: 3-D far-field gain of 4×1 PIFA array antenna

Effect of Changing Width (W)

Now let's select the microstrip patch antenna, which has preferable performance, with RT5880 substrate having dielectric constant $\epsilon_r = 2.2$ for this analysis. In this analysis the height of the patch is kept fixed at 0.2 mm and the length of the patch is also kept fixed at 3.5 mm, then the width of the patch is varied as (4.0, 4.1, 4.2, 4.3, 4.4,) mm. The characteristic parameters of proposed antenna in terms of directivity, return loss, bandwidth and efficiencies is tabulated in the following Table 4.3.

As varying values of the patch width, the simulation result shows there is no significant change on directivity, radiation efficiency and bandwidth.

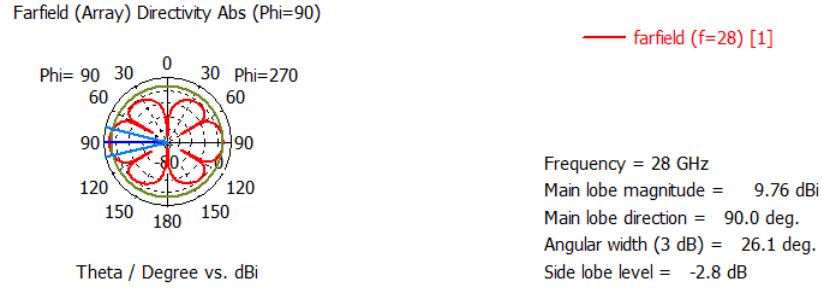


Figure 4.27: 3-D polar plot of 4×1 PIFA array antenna

Width (mm)	W = 4.0	W = 4.1	W = 4.2	W = 4.3	W = 4.4
Gain (dBi)	12.24	12.23	12.20	12.19	12.17
Directivity (dBi)	12.43	12.42	12.41	12.40	12.39
Tot. efficiency (dB)	-3.54	-3.69	-3.89	-4.05	-4.28
Rad. efficiency (dB)	-0.19	-0.196	-0.209	-0.216	-0.228
Return Loss (dB)	-38.83	-43.65	-32.55	-27.98	-24.79
Bandwidth (GHz)	0.76	0.74	0.731	0.727	0.724

Table 4.3: Effect of the patch width

Effect of Changing Length (L)

In Table 4.4 observation, the dielectric constant, height of the substrate and width of the patch are kept fixed at 2.2, 0.2 mm and 4.2 mm, respectively and the length of the patch is varied as (3.3, 3.4, 3.5, 3.6, 3.7) mm.

Length (mm)	L = 3.3	L = 3.4	L = 3.5	L = 3.6	L = 3.7
Gain (dBi)	12.32	12.40	12.18	11.79	11.29
Directivity (dBi)	12.45	12.53	12.40	12.11	11.64
Tot. efficiency (dB)	-0.29	-1.13	-4.09	-6.40	-8.24
Rad. efficiency (dB)	-0.127	-0.125	-0.21	-0.318	-0.352
Return Loss (dB)	-19.29	-23.28	-32.55	-42.06	-26.97
Bandwidth (GHz)	0.691	0.721	0.731	0.717	0.706

Table 4.4: Effect of the patch length

Different simulation result is observed by varying the length. As the length increases there is no significant change in the bandwidth. At length below 3.5mm there is no significant variation in the directivity and radiation efficiency obtained.

Effect of Changing Substrate Thickness

Selection of appropriate substrate thickness is another significant task in microstrip patch antenna design. To choose appropriate substrate thickness (h), a designer needs to know the effect of changing substrate thickness on the different antenna parameters. In Table 4.5, the antenna parameters are compared by shifting substrate thickness (h) from 0.1 mm to 0.3 mm and the width and length of patch are kept fixed at 4.2 mm and 3.5 mm, respectively for rectangular microstrip patch antenna.

From the comparison data of Table 4.5, it is seen that with increasing the substrate height the directivity of the antenna decreases but the bandwidth increases and a better return loss performance from ($h=0.1$ to $h=0.2$).

Height (mm)	H = 0.1	H = 0.15	H = 0.2	H = 0.25	H = 0.3
Gain (dBi)	12.14	12.09	12.18	12.15	12.01
Directivity (dBi)	12.49	12.37	12.40	12.32	12.15
Tot. efficiency (dB)	-5.21	-4.54	-4.09	-3.89	-3.71
Rad. efficiency (dB)	-0.35	-0.28	-0.21	-0.16	-0.14
Return Loss (dB)	-14.95	-27.37	-32.55	-20.37	-26.45
Bandwidth (GHz)	0.37	0.58	0.71	0.81	0.85

Table 4.5: Effect of the substrate thickness

In the above analysis the effect of the antenna parameters on millimeter wave antenna performance is done and the results have been obtained and discussed. It can be presumed that, corruption of antenna performance results but size of the antenna reduces due to the use of substrate material with higher dielectric constant in microstrip patch antenna design. With increasing substrate thickness (h), the bandwidth of the antenna is enhanced with taking into account small reduction in the directivity. The bandwidth can be enhanced by increasing the substrate thickness and decreasing the permittivity of substrate.

CHAPTER V

CONCLUSION AND RECOMMENDATION FOR FUTURE WORK

5.1 Conclusion

In this thesis a printed dipole, microstrip patch and PIFA antenna arrays have been designed and simulated using CST Microwave Studio software for mobile communication. These antennas can be mounted on the surface of handheld cell phones. Antennas at 28 GHz are required to achieve high data rate for the next generation of mobile communication systems. They should have a high gain to overcome the high path loss at mm-wave frequencies. The high gain antenna provides a wide coverage area for data exchange. Since the gain obtained by array procedure is much higher than that of single element antenna, an array antenna of four elements aiming for 5G mobile communications is used in this thesis. The radiation pattern and other important parameters such as gain, return loss, efficiency, directivity and VSWR have been studied to analyze their performances at an operating frequency of 28 GHz.

Comparison between a printed dipole antenna, patch antenna and planar inverted-F antenna using the simulation results have been carried out. Based on the results obtained 4×1 array antennas have maximum gain and directivity of 9.87 dBi and 10.12 dBi for printed dipole antenna, 12.09 dBi and 12.37 dBi for microstrip patch antenna, and 9.79 dBi and 9.812 dBi for PIFA, respectively. The VSWR and return loss value, respectively, is found to be 2.4 and -7.57 dB for printed dipole array antenna, 1.09 and -27.37 dB for microstrip patch array antenna, and 2.6 and -6.5 dB for array of PIFA. The radiation efficiency for printed dipole array antenna is -0.248, for microstrip patch array antenna is -0.275, and for array of PIFA is -0.18. In this regard, it is revealed that the microstrip patch antennas are quite capable of achieving the highest performances and represent an obvious choice for

mobile applications due to their low fabrication cost, lightweight and volume, a low-profile configuration and highest performance results as compared to the other types of antennas.

From this thesis, it is also clear that the dielectric constant and height of substrate material have significant effect on the performance of a rectangular microstrip patch antenna. In this design use of substrate material with higher value of dielectric constant results degradation of antenna performance, such as lower gain and bandwidth, but size of the antenna reduces. Less substrate thickness results better gain and directivity but the bandwidth of the antenna is decreased.

5.2 Recommendation for Future Work

The following areas of study are worthy of consideration to carry out further study.

First, an experimental demonstration of the effect of a person, hand- and body-effect, on the signal propagation between the transmitter and the receiver should be presented in the future work.

Moreover, the researcher can increase the array size to further improve the antenna performance.

Finally, it is recommended to develop practical infrastructure of the above designed antenna systems.

BIBLIOGRAPHY

- [1] J. Helander, D. Sjöberg, M. Gustafsson, K. Zhao, and Z. Ying, “Characterization of millimeter wave phased array antennas in mobile terminal for 5g mobile system.” *IEEE*, 2015, pp. 7–8.
- [2] C. A. Balanis, “Antenna theory, hoboken,” *New Jersey: John Wiley & Sons, Inc*, vol. 8, pp. 21–31, 2005.
- [3] D. Gupta, A. Duvey, and S. Agrawal, “A review: Microstrip antenna,” 2019.
- [4] F. Redzwan, M. Ali, M. M. Tan, and N. Miswadi, “Design of planar inverted f antenna for lte mobile phone application,” in *2014 IEEE REGION 10 SYMPOSIUM*. *IEEE*, 2014, pp. 19–22.
- [5] T. J. Pradeep and G. Kalaimagal, “Design of 4×2 corporate feed microstrip patch antenna using inset feeding technique with defective ground plane structure,” in *Artificial Intelligence and Evolutionary Computations in Engineering Systems*. Springer, 2017, pp. 269–283.
- [6] W. L. Stutzman and G. A. Thiele, *Antenna theory and design*. John Wiley & Sons, 2012.
- [7] M. S. Sharawi, “Use of low-cost patch antennas in modern wireless technology,” *IEEE Potentials*, vol. 25, no. 4, pp. 35–47, 2006.
- [8] W. Roh, J.-Y. Seol, J. Park, B. Lee, J. Lee, Y. Kim, J. Cho, K. Cheun, and F. Aryanfar, “Millimeter-wave beamforming as an enabling technology for 5g cellular communications: Theoretical feasibility and prototype results,” *IEEE communications magazine*, vol. 52, no. 2, pp. 106–113, 2014.
- [9] B. Bangerter, S. Talwar, R. Arefi, and K. Stewart, “Networks and devices for the 5g era,” *IEEE Communications Magazine*, vol. 52, no. 2, pp. 90–96, 2014.
- [10] A. Obot, O. Simeon, and J. Afolayan, “Comparative analysis of path loss prediction models for urban macrocellular environments,” *Nigerian journal of technology*, vol. 30, no. 3, pp. 50–59, 2011.
- [11] M. H. Habaebi, M. Janat, M. R. Islam, and B. Hamida, “Phased array antenna meta-material based design operating in millimeter wave for 5g mobile networks,” in *2016 IEEE Student Conference on Research and Development (SCORED)*. *IEEE*, 2016, pp. 1–4.
- [12] J. Helander, K. Zhao, Z. Ying, and D. Sjöberg, “Performance analysis of millimeter-wave phased array antennas in cellular handsets,” *IEEE Antennas and Wireless Propagation Letters*, vol. 15, pp. 504–507, 2015.

- [13] D. Anjali and A. Kaur, "Performance analysis of patch and pifa antenna for wcs and sdr applications," *International Journal of Advanced Research in Computer and Communication Engineering*, vol. 6, no. 7, pp. 265–269, 2017.
- [14] K. P. Simon, *Foundations of Antenna Engineering: A Unified Approach for Line-of-Sight and Multipath*. Chalmers University of Technology, 2017.
- [15] L. C. Godara, *Smart antennas*. CRC press, 2004.
- [16] Newell, M. Tuley, E. Gillespie, H. G. Oltman, E. Urbanik, E. Hart, A. D. Olver, A. Villeneuve, Reilly, D. F. Franklin, I. N. Knight, R. H. Reimer, R. García, and J. L. Koepfinger, "Ieee standard definitions of terms for antennas," *IEEE Std 145-1993*, pp. 1–32, 1993.
- [17] S. N. Makarov *et al.*, *Antenna and EM Modeling with MATLAB*. Wiley-interscience New York, NY, 2002.
- [18] N. Chavda, D. Vedvyas, and P. Kiran, "Designing of microstrip patch antenna for 3g-wcdma applications," *International Advanced Research Journal in Science, Engineering and Technology*, vol. 1, pp. 49–53, 2012.
- [19] A. Fatthi Alsager, "Design and analysis of microstrip patch antenna arrays," 2011.
- [20] S. X. Ta, H. Choo, and I. Park, "Broadband printed-dipole antenna and its arrays for 5g applications," *IEEE Antennas and Wireless Propagation Letters*, vol. 16, pp. 2183–2186, 2017.
- [21] S. X. Ta and I. Park, "Cavity-backed angled-dipole antennas for millimeter-wave wireless applications," *International Journal of Antennas and Propagation*, vol. 2016, 2016.
- [22] M. Scott, "A printed dipole for wide-scanning array application," 2001.
- [23] R. P. Ghosh, B. Gupta, and S. Chowdhury, "Broadband printed dipole antennas with shaped ground plane," in *TENCON 2010-2010 IEEE Region 10 Conference*. IEEE, 2010, pp. 416–421.
- [24] R. Gahley and B. Basu, "A time modulated printed dipole antenna array for beam steering application," *International Journal of Antennas and Propagation*, vol. 2017, 2017.
- [25] Y. S. Khraisat, "Design of 4 elements rectangular microstrip patch antenna with high gain for 2.4 ghz applications," *Modern applied science*, vol. 6, no. 1, p. 68, 2012.
- [26] S. K. Sidhu and J. S. Sivia, "Comparison of different types of microstrip patch antennas," *International Journal of Computer Applications*, vol. 975, p. 8887, 2015.
- [27] R. Garg, P. Bhartia, I. J. Bahl, and A. Ittipiboon, *Microstrip antenna design handbook*. Artech house, 2001.

- [28] M. T. I.-u. Huque, M. S. Islam, M. F. Samad, and M. K. Hosain, "Design and performance analysis of the rectangular spiral microstrip antenna and its array configuration," in *Proceedings of the 9th International Symposium on Antennas, Propagation and EM Theory*. IEEE, 2010, pp. 219–221.
- [29] S. Nikita, J. Bhawana, S. Pradeep, and P. Ranjan, "Rectangular patch micro strip antenna: A survey," *IARJSET*, vol. 1, pp. 144–147, 2014.
- [30] R. C. Johnson and H. Jasik, "Antenna engineering handbook," *New York, McGraw-Hill Book Company, 1984, 1356 p. No individual items are abstracted in this volume.*, 1984.
- [31] R. Z. Syeda, "Design and performance analysis of switched beam series-fed patch antenna array for 60ghz wpan applications," Master's thesis, Universitat Politècnica de Catalunya, 2014.
- [32] J. M. Rathod, "Design development of antenna for tvtransmission for connecting outdoor broadcastsvan to the studio for rural areas," *International Journal of Computer and Electrical Engineering*, vol. 2, no. 2, p. 251, 2010.
- [33] P. S. Nakar, "Design of a compact microstrip patch antenna for use in wireless/cellular devices," 2004.
- [34] G. Kumar and K. P. Ray, *Broadband microstrip antennas*. Artech house, 2003.
- [35] H. Wang and I. Park, "Series-fed printed dipole array antenna," in *2018 11th Global Symposium on Millimeter Waves (GSMM)*. IEEE, 2018, pp. 1–3.
- [36] J. Y. Pang, S. Q. Xiao, Z. F. Ding, and B. Z. Wang, "Two-element pifa antenna system with inherent performance of low mutual coupling," *IEEE Antennas and Wireless Propagation Letters*, vol. 8, pp. 1223–1226, 2009.
- [37] D. S. Raghavan and N. Jayanthi, "Design of planar inverted-f antenna for wireless application," *WSEAS Transactions on communications*, vol. 8, no. 8, pp. 863–872, 2009.
- [38] M. El Halaoui, A. Kaabal, H. Asselman, S. Ahyoud, and A. Asselman, "Multiband planar inverted-f antenna with independent operating bands control for mobile handset applications," *International Journal of Antennas and Propagation*, vol. 2017, 2017.
- [39] D. M. Pozar, *Microwave engineering*. John Wiley & Sons, 2009.
- [40] T. A. Milligan, *Modern antenna design*. John Wiley & Sons, 2005.
- [41] H. J. Visser, *Array and phased array antenna basics*. John Wiley & Sons, 2006.
- [42] F. Redzwan, M. Ali, M. M. Tan, and N. Miswadi, "Design of planar inverted f antenna for lte mobile phone application," in *2014 IEEE REGION 10 SYMPOSIUM*. IEEE, 2014, pp. 19–22.

APPENDIX

SAMPLE DESIGN AND ANALYSIS PROCEDURE USING COMPUTER SIMULATION TECHNIQUE (CST) STUDIO SUITE

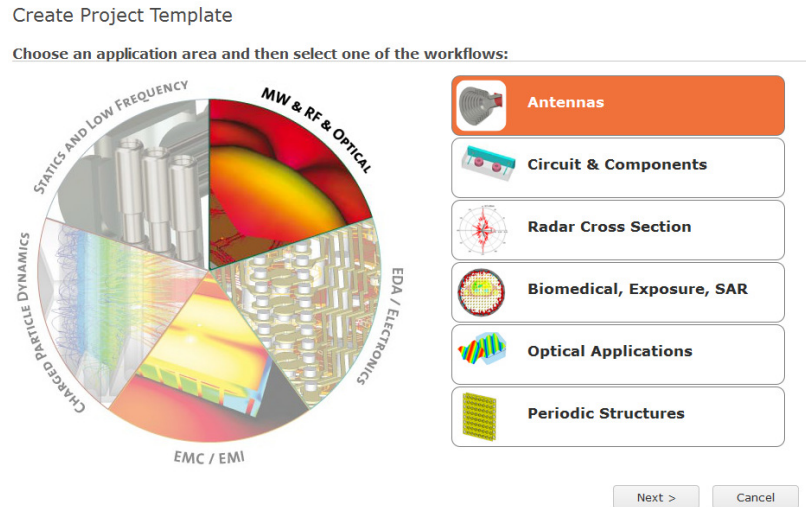
CST microwave studio (CST MWS) is a pro instrument for the 3D EM simulation of high frequency components. CST MWS empowers the fast and accurate analysis of high frequency (HF) devices such as antennae, filters, couplers, planar and multi-layer structures and SI and EMC effects which makes it the first choice in technology leading research and development. CST software makes accessible time domain and frequency domain solvers, CST MWS offers further solver modules for explicit applications. Filters for the import of specific CAD files and the extraction of SPICE parameters can enhance design possibilities and also save time.

For design the different antennas we follow the next steps:

Step 1: Open CST Studio Suite. Then select and open CST Microwave Studio (new project template):



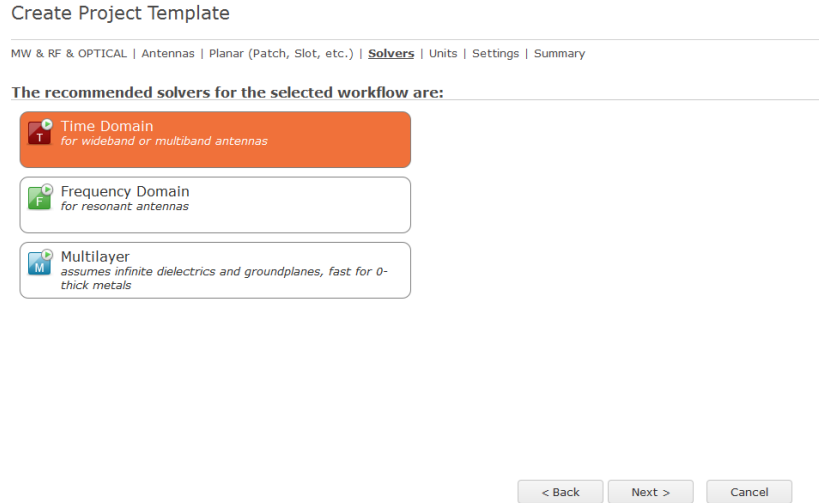
Step 2: Select 'Antennas' template from the 'MW & RF & OPTICAL' application area:



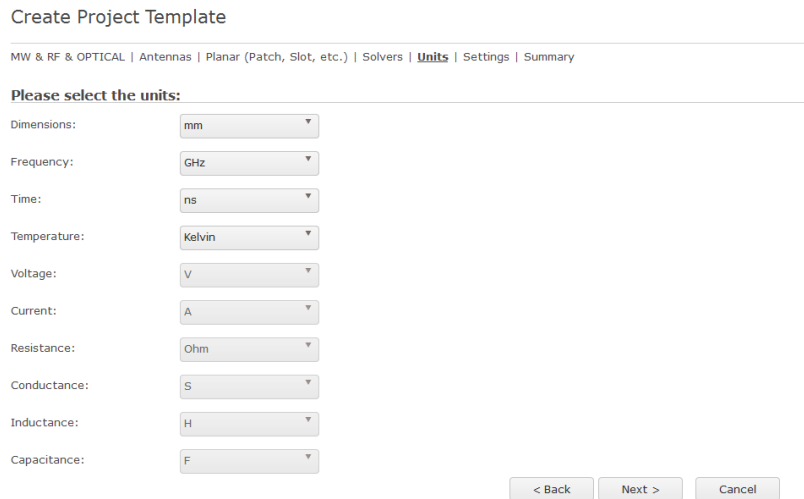
Step 3: Select the most convenient option for the analysis of a wire antennas. The software will give some initial parameters which are commonly used for this type of antennas.



Step 4: To select the recommended solver for the work-flow follow the indications of the quick start:



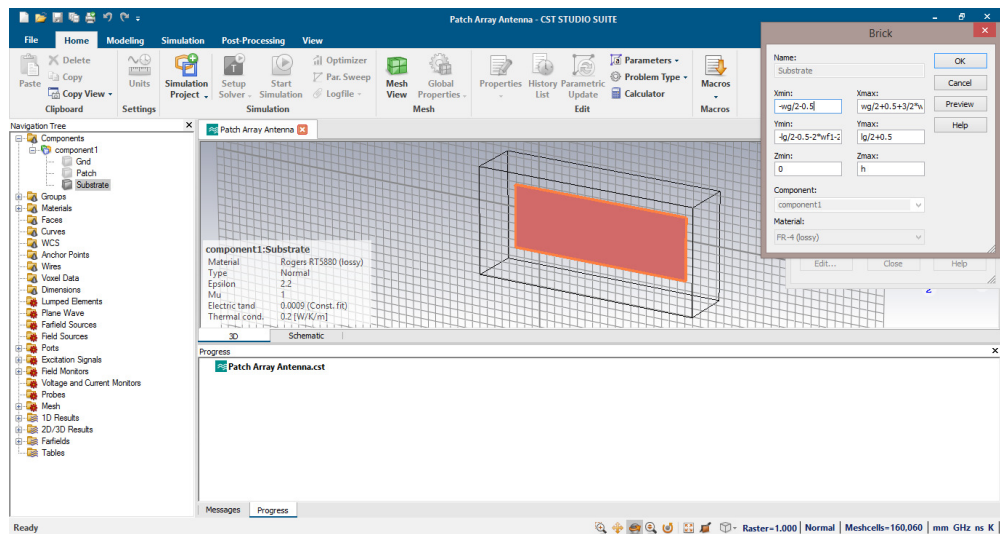
Step 5: Define the units: Typically "mm" for the lengths, "GHz" for the frequency, and "ns" for the time analysis. Other unites are also listed on the figure below.



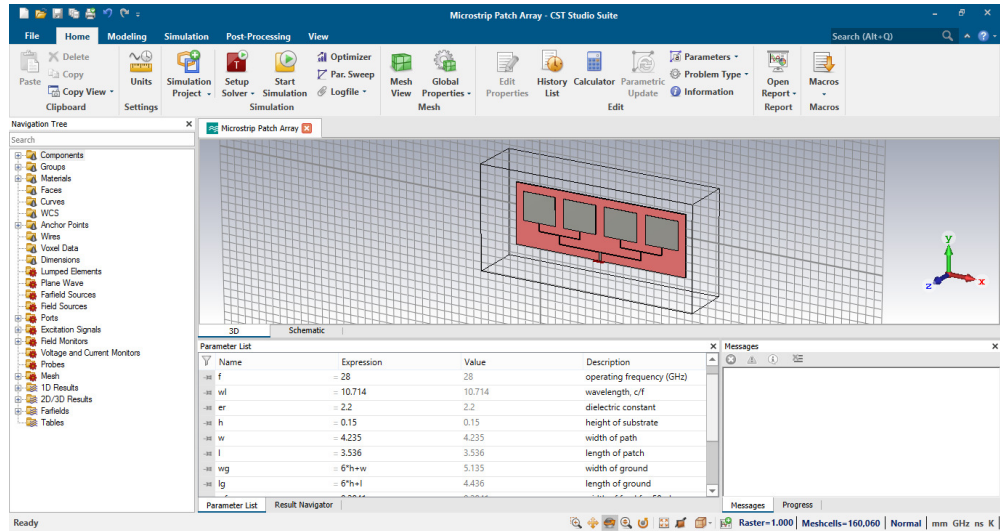
Step 6: Define the frequency of study and the monitors: The frequency will be set from 26 GHz to 30 GHz. Then visualize the electric fields and the far fields at the central frequency of 28 GHz.



Step 7: Set the parameters and design the antenna:



Step 8: After finalizing the antenna design start the simulation:



Step 9: Displaying the simulation results:

From the simulation results the S-parameters, radiation pattern, gain and directivity can be shown.

